

Characteristics of Ginsenoside Rg₃-Mediated Brain Na⁺ Current Inhibition

JUN-HO LEE[§], SANG MIN JEONG[§], JONG-HOON KIM, BYUNG-HWAN LEE, IN-SOO YOON, JOON-HEE LEE, SUN-HYE CHOI, DONG-HYUN KIM, HYEWHON RHIM, SUNG SOO KIM, JAI-IL KIM, CHOON-GON JANG, JIN-HO SONG AND SEUNG-YEOL NAH

Research Laboratory for the Study of Ginseng Signal Transduction and Department of Physiology, College of Veterinary Medicine, Konkuk University, Seoul Korea, 143-701 (J.-H. L., S.M.J., J.-H.K., B.-H.L., I.-S.Y., J.-H.L., S.-H.C., S.-Y.N); College of Pharmacy, KyungHee University, Seoul Korea 130-701 (D.-H.K.); Biomedical Research Center, KIST, Seoul Korea 136-701 (H.R.); Korea Food Research Institute, Korea 483-746 (S.-S.K.); Department of Life Science, KJIST, Kwangju, Korea (J.-I.K); Department of Pharmacology, College of Pharmacy Sungkyunkwan University, Korea 440-746 (C.-G.J.); and Department of Pharmacology, College of Medicine, Chung-Ang University, Seoul Korea 156-756 (J.-H.S.)

Running Title

Ginsenoside Rg₃ Blocks Brain Na⁺ Channels

[§]Both authors contributed equally to this work.

***Correspondence to:**

Prof. Seung-Yeol Nah, Research Laboratory for the Study of Ginseng Signal Transduction and Dept. of Physiology, College of Veterinary Medicine, Konkuk University, Seoul 143-701, Korea.

Email: synah@konkuk.ac.kr

Manuscript information

The number of text pages: 36

The number of table: 1

The number of figures: 10

The number of words in abstract: 250

The number of words in introduction: 664

The number of words in discussion: 1378

ABSTRACT

We previously demonstrated that ginsenoside Rg₃ (Rg₃), an active ingredient of *Panax ginseng*, inhibits brain-type Na⁺ channel activity. Here, we sought to elucidate the molecular mechanisms underlying Rg₃-induced Na⁺ channel inhibition. We used the two-microelectrode voltage clamp technique to investigate the effect of Rg₃ on Na⁺ currents (*I*_{Na}) in *Xenopus* oocytes expressing wild-type rat brain Na_v1.2 α and β 1 subunits, or mutants in the channel entrance, the pore region, the lidocaine/TTX binding sites, the S4 voltage sensor segments of domains I to IV, and the IFM inactivation cluster. In oocytes expressing wild-type Na⁺ channels, Rg₃ induced tonic and use-dependent inhibitions of peak *I*_{Na}. The Rg₃-induced tonic inhibition of *I*_{Na} was voltage-dependent, dose-dependent and reversible, with an IC₅₀ value of 32 \pm 6 μ M. Rg₃ treatment produced a 11.2 \pm 3.5 mV depolarizing shift in the activation voltage, but did not alter the steady-state inactivation voltage. Mutations in the channel entrance, pore region, lidocaine/TTX binding sites or voltage sensor segments did not affect Rg₃-induced tonic blockade of peak *I*_{Na}. However, Rg₃ treatment inhibited the peak and plateau *I*_{Na} in the IFMQ3 mutant, indicating that Rg₃ inhibits both the resting and open states of Na⁺ channel. Neutralization of the positive charge at position 859 of voltage sensor segment domain II abolished the Rg₃-induced activation voltage shift and use-dependent inhibition. These results reveal that Rg₃ is a novel Na⁺ channel inhibitor capable of acting on the resting and open states of Na⁺ channel via interactions with the S4 voltage-sensor segment of domain II.

Introduction

Na⁺ channels are transmembrane proteins that consist of a pore-forming α subunit and auxiliary β 1, β 2 and β 3 subunits (Catterall, 1987; Goldin, 1995; Wang et al., 2003). The α subunit is composed of four homologous domains (I-IV), each composed of six α -helical transmembrane segments (S1-S6). Among them, the S4 segment acts as the voltage-sensing apparatus of Na⁺ channel (Hodgkin and Huxley, 1952). The pore-forming α subunit is responsible for voltage-dependent increases in Na⁺-selective permeability. These changes trigger the inward Na⁺ current (I_{Na}) that initiates axonal and somatic action potentials in nerve and muscle fibers, and may also be involved in axonal information transfer for intraneuronal or interneuronal communications (Hodgkin and Huxley, 1952; Stuart and Sakmann, 1994). Na⁺ channels can exist in resting (closed), open (active) or inactivated states, and transition among the various states in response to time- and voltage-dependent signaling (Hodgkin and Huxley, 1952). Various drugs can exhibit differential affinities to the specific Na⁺ channel states. For example, lidocaine (a local anesthetic) and phenytoin (an anti-convulsant) show a low affinity for the resting state and a higher affinity for the inactivated state, whereas flecainide (an anti-arrhythmic drug) inhibits the open state (Hondegam and Kazung, 1984; Bean et al., 1983). Na⁺ channel modulators that act as drugs and/or neurotoxins often affect both permeation and gating properties (Goldin, 1995), and site-directed mutagenesis studies have allowed characterization of the detailed action and binding sites of various drugs and toxins that regulate neuronal Na⁺ channel activity (Catterall, 1987; Goldin, 1995; Wang et al., 2003).

Ginseng, the root of *Panax ginseng* C.A. Meyer, is well known in herbal

medicine as a tonic and restorative agent. The main molecular ingredients responsible for the actions of ginseng are the ginsenosides (also called ginseng saponins), which are amphiphilic molecules comprising a hydrophobic backbone of aglycone (a hydrophobic four-ring steroid-like structure) linked to hydrophilic carbohydrate side chains consisting of monomers, dimers or tetramers (Fig. 1). The ginsenosides are classified as protopanaxadiol or protopanaxatriol, according to the positions of the carbohydrate moieties at carbons -3, -6 and -20, which can be either free or connected to sugar rings (Nah, 1997). We recently demonstrated that ginsenoside Rg₃ (20-*S*-protopanaxadiol-3-[O-β-D-glucopyranosyl (1→ 2)-β-glucopyranoside]) (Rg₃), one of the active ingredients in *Panax ginseng*, inhibits voltage-dependent brain Na⁺ channel activity expressed in *Xenopus laevis* oocytes (Jeong et al., 2004; Kim et al., 2005). However, no previous work has examined the underlying mechanisms by which Rg₃ regulates Na⁺ channel currents.

We herein sought to characterize ginsenoside-mediated Na⁺ channel regulation in a *Xenopus* oocyte gene expression system. This model system has few endogenous ion channels (Dascal, 1987) and allows heterologous expression of ion channels for various biochemical studies (Choi et al, 2002; Choi et al., 2003; Sala et al., 2002). We expressed brain Na⁺ channels by intraoocyte injection of cRNAs encoding the Na_v1.2 α and β1 subunits (Pugsley and Goldin, 1998; Pugsley et al., 2000) with or without various mutations, and examined the changes in *I*_{Na} in response to Rg₃ treatment. We found that Rg₃ caused both tonic and use-dependent inhibitions of the peak *I*_{Na} following low- and high-frequency stimulations. We further found that mutations in the channel pore entrance, pore region, lidocaine binding sites, TTX binding sites, and S4 voltage sensor

segments of domains I-IV of the Na^+ channel had no effect on Rg_3 -induced tonic inhibition of peak I_{Na} . However, when inactivation cluster I1488-F1489-M1490 was mutated to I1488Q-F1489Q-M1490Q (IFMQ3) (West et al., 1992) to create an inactivation-deficient mutant, Rg_3 treatment inhibited both the peak and non-inactivating plateau I_{Na} levels of this mutant, indicating that Rg_3 regulates the resting and open states of the expressed Na^+ channel. A single K to Q mutation at residue 859 (K859Q) within the S4 voltage sensor segment of domain II abolished the Rg_3 -induced shift of the activation voltage and use-dependent inhibition, while changes in the other domains did not. Taken together, these results show for the first time that Rg_3 acts as a novel Na^+ channel blocker by interacting with the S4 voltage-sensor segment of domain II.

Experimental Procedures

Materials. The 20(S)-ginsenoside, Rg_3 (Fig. 1) was kindly provided by the Korean Ginseng Cooperation (Taejon, Korea). The cDNA for the rat brain Na^+ channel $\text{Na}_v1.2$ α subunit was kindly provided by Dr. A. L. Goldin (University of California, Irvine, CA, USA) and that for the Na^+ channel $\beta 1$ subunit was kindly provided by Dr. T. Zimmer (Friedrich Schiller University, Jena, Germany). Other agents were purchased from Sigma (St. Louis, MO, USA).

Preparation of *Xenopus* oocytes and microinjection. *Xenopus laevis* frogs were purchased from Xenopus I (Ann Arbor, MI, USA). Their care and handling was in accordance with the highest standards of institutional guidelines. For isolation of oocytes, frogs were anesthetized with an aerated solution of 3-amino benzoic acid ethyl

ester and ovarian follicles were removed. The oocytes were separated by treatment with collagenase and agitation for 2 h in Ca^{2+} -free medium containing 82.5 mM NaCl, 2 mM KCl, 1 mM MgCl_2 , 5 mM HEPES, 2.5 mM sodium pyruvate, 100 units/ml penicillin and 100 $\mu\text{g/ml}$ streptomycin. Stage V-VI oocytes were collected and stored in ND96 (96 mM NaCl, 2 mM KCl, 1 mM MgCl_2 , 1.8 mM CaCl_2 , and 5 mM HEPES, pH 7.5) supplemented with 0.5 mM theophylline and 50 $\mu\text{g/ml}$ gentamicin. This oocyte-containing solution was maintained at 18°C with continuous gentle shaking and renewed everyday. Electrophysiological experiments were performed within 5-6 days of oocyte isolation, with chemicals applied to the bath. For Na^+ channel experiments, 40 nl of cRNAs encoding the $\text{Nav}1.2$ α and $\beta 1$ subunits was injected into the animal or vegetal pole of each oocyte one day after isolation, using a 10 μl VWR microdispenser (VWR Scientific, San Francisco, CA, USA) fitted with a tapered glass pipette tip (15-20 μm in diameter) (Choi et al., 2003).

Site-directed mutagenesis of $\text{Nav}1.2$ and *in vitro* transcription of Na^+ channel subunit cDNAs. The substitutions mutations of single or triplet amino acids were performed using the QuikChange™ XL Site-Directed Mutagenesis Kit (Stratagene, La jolla, CA, USA), along with Pfu DNA polymerase and mutated sense and antisense primers. Overlap extension of the target domain by sequential polymerase chain reactions was carried out according to the manufacturer's recommended protocol. The final PCR products were transformed to *E. coli* strain DH5 α , screened by PCR and confirmed by DNA sequencing of the target region. The mutant DNA constructs were linearized at the 3' end by *NotI* digestion, and run-off transcripts were prepared using methylated cap analog, $\text{m}^7\text{G}(5')\text{ppp}(5')\text{G}$. The cRNAs were prepared using the

mMessage mMachine transcription kit (Ambion, Austin, TX, USA) with T7 RNA polymerase. The absence of degraded RNA was determined by denaturing agarose gel electrophoresis followed by ethidium bromide staining. Similarly, recombinant plasmids containing wild-type Nav1.2 α or β 1 subunit cDNA inserts were linearized by digestion with the appropriate restriction enzymes, and cRNAs were obtained using the mMessage mMachine *in vitro* transcription kit (Ambion, Austin, TX, USA) with SP6 RNA or T7 polymerases. The final cRNA products were resuspended at a concentration of 1 μ g/ μ l in RNase-free water, and stored at -80°C until use (Choi et al., 2003).

Data recording. A custom-made Plexiglas net chamber was used for two-electrode voltage-clamp recordings. The chamber was constructed by milling two concentric wells into the chamber bottom (the diameter/height of the upper well was 8/3 mm and that of the lower well was 6/5 mm) and gluing plastic meshes (~ 0.4 mm grid diameter) onto the bottom of the upper well. A perfusion inlet (~ 1 mm in diameter) was drilled through the wall of the lower well, and a suction tube was placed on the edge of the upper well. For experiments, a single oocyte was placed on the net separating the upper and lower wells. The net grids helped anchor the oocyte in place during the electrophysiological recordings. The oocyte was then impaled with two microelectrodes filled with 3 M KCl (0.2-0.7 $\text{M}\Omega$) and electrophysiological experiments were carried out at room temperature using an Oocyte Clamp (OC-725C, Warner Instruments, (Hamden, CT, USA). Stimulation and data acquisition were controlled with a pClamp 8 (Axon Instruments, Union City, CA, USA) (Choi et al., 2003). For most of the electrophysiological experiments on Na^{+} channel activity, oocytes were clamped at a holding potential of -100 mV and the membrane potential was depolarized to -10 mV

for 100 ms every 5 s. Linear leak currents were corrected by means of the leak subtraction procedure (Jeong et al., 2005).

The voltage-dependence of Na^+ channel activation was calculated by measuring the peak current at test potentials ranging from -50 mV to $+50$ mV evoked in 5 mV increments. The conductance (g_{Na}) was calculated according to the equation, $g_{\text{Na}} = I_{\text{Na}}/(V_g - V_r)$, where I_{Na} is the peak amplitude of the Na^+ current, V_g is the test potential, and V_r is the reversal potential for Na^+ . The conductance-voltage curves were drawn according to the equation $g_{\text{Na}}/\text{max}g_{\text{Na}} = 1/\{1 + \exp [(V_{g0.5} - V_g)/kg]\}$, where $\text{max}g_{\text{Na}}$ is the maximum value for g_{Na} , $V_{g0.5}$ is the potential at which g_{Na} is $0.5\text{max}g_{\text{Na}}$, and kg is the slope factor (potential required for an e -fold change). The voltage-dependence of Na^+ channel inactivation was determined using 200 ms conditioning pre-pulses ranging from -60 mV to $+20$ mV from a holding potential of -100 mV in 5 mV increments, followed by a test pulse to -10 mV for 5 ms. The peak I_{Na} was normalized to its respective maximum value ($\text{max}I_{\text{Na}}$) and plotted as a function of the pre-pulse potential. The steady-state inactivation curves were drawn according to the equation $I_{\text{Na}}/\text{max}I_{\text{Na}} = 1/\{1 + \exp [(V_h - V_{h0.5})/kh]\}$, where V_h is pre-pulse potential, $V_{h0.5}$ is the potential at which I_{Na} is $0.5\text{max}I_{\text{Na}}$, and kh is the slope factor.

The frequency-dependent effect of Rg_3 was examined using a protocol in which 50 depolarizing pulses of 10 ms duration and 10 Hz frequency were applied to -10 mV from a holding potential of -100 mV. The protocol was run in the absence (control) and presence of Rg_3 (10 or 100 μM). The current amplitude of each pulse was normalized to the peak maximal current (pulse number 1) and plotted as a function of pulse number.

The kinetics of the Rg_3 blockade of IFMQ3, which is the fast inactivation deficient mutant of $\text{Nav}1.2$, were examined by clamping oocytes at -100 mV in ND96 solution. A

single 500 ms depolarizing pulse to -10 mV was applied and the I_{Na} was recorded. Different concentrations of Rg₃ (10, 30, 100 or 300 μ M) were perfused into the bath for 1 min, and a second, single depolarizing pulse from -100 mV to -10 mV was given. The data were individually fit to either a single $[1-A_{\text{slow}}*\exp(-t/\tau_{\text{slow}})]$ or double $[1-A_{\text{fast}}*\exp(-t/\tau_{\text{fast}})] + [1-A_{\text{slow}}*\exp(-t/\tau_{\text{slow}})]$ exponential equation, in which A_{fast} and A_{slow} represent the proportion of current decaying with time constants τ_{fast} and τ_{slow} , respectively, and t is the time interval. If we assume that a first order relationship describes the dependence of the blocking rate on the concentration of the blocking chemical, the apparent rate constant for binding (k_{on}) can be obtained by fitting the τ_{fast} values with the equation: $1/\tau_{\text{fast}} = k_{\text{on}}*[Rg_3] + l$ (Lansman et al., 1986). Recovery from open channel blockade was measured at a holding potential of -100 mV with a 10 ms depolarizing pre-pulse to -10 mV (P1) followed by a variable recovery period from 10 ms to 500 ms, subsequently followed by a 10 ms test pulse to -10 mV (P2).

Data analysis. To obtain the concentration-response curve of the effect of Rg₃ on I_{Na} , the peak amplitudes at different concentrations of Rg₃ were plotted, and then fitted to the following Hill equation using the Origin software (Origin, Northampton, MA, USA): $y/y_{\text{max}} = [A]^{nH}/([A]^{nH} + [EC_{50}]^n)$, where y is the peak I_{Na} at given concentration of Rg₃, y_{max} is the maximal peak I_{Na} , EC_{50} is the concentration of Rg₃ producing a half-maximum effect, $[A]$ is the concentration of Rg₃, and nH is the interaction coefficient. All values are presented as means \pm S.E.M. The differences between the means of control and treatment values were determined using an unpaired Student's t -test. A value of $P < 0.05$ was considered statistically significant.

Results

The effect of Rg₃ on peak I_{Na} in oocytes expressing Nav1.2. The effect of Rg₃ on currents from brain Na⁺ channels expressed in *Xenopus* oocytes was examined. I_{Na} was recorded by two-electrode voltage clamping of oocytes injected with cRNAs encoding Nav1.2 α and β 1 subunits. Oocytes were held at –100 mV, and I_{Na} was elicited by depolarization to –10 mV at a low frequency (0.2 Hz). This procedure minimized the use-dependent blockade and allowed evaluation of whether Rg₃ produced a tonic blockade of peak I_{Na} (Pugsley and Goldin, 1998; Pugsley et al., 2000). For comparison, we also examined the effect of lidocaine on the peak I_{Na} . As shown in Figure 2A, the depolarizing voltage step induced a large inward I_{Na} with rapid inactivation. Application of Rg₃ (100 μ M) or lidocaine (1000 μ M) inhibited the peak I_{Na} by 64 ± 7 and $41 \pm 10\%$, respectively (Fig. 2A, *inset*), indicating that both agents induced a tonic inhibition of the Na⁺ current.

Concentration-dependent inhibition of I_{Na} by Rg₃ or lidocaine. The current-voltage relationships were assessed in the absence or presence of Rg₃ with voltage steps ranging from –50 to +50 mV evoked from a holding potential of –100 mV every 5 s. As shown in Figure 2B, addition of Rg₃ caused a voltage-dependent reduction in peak I_{Na} , with a more pronounced reduction noted at lower voltage ranges. In addition, Rg₃ treatment shifted the threshold voltage of channel opening and the voltage of the peak I_{Na} to more depolarized values compared to the control. However, Rg₃ had no significant effect on the kinetics of current decay. As shown in Figure 2C, the inhibitory effect of Rg₃ on peak I_{Na} was dose-dependent up to 300 μ M, with an estimated IC₅₀ value of 32 ± 6 μ M. The Hill coefficient was 1.1 ± 0.4 , indicating that one molecule of Rg₃ appeared

sufficient to block one Na^+ channel. We also tested the effect of lidocaine on peak I_{Na} , and found that it was dose-dependent up to 3000 μM (Fig. 2C). The IC_{50} was $966 \pm 37 \mu\text{M}$, which is consistent with previous report (Pugsley and Goldin, 1998). These findings indicate that Rg_3 was more potent than lidocaine by about 33.2-fold. Interestingly, the IC_{50} value for Rg_3 -mediated Na^+ current inhibition was 2-fold higher than that for Rg_3 -induced inhibition of Na^+ influxes triggered by acetylcholine treatment in bovine adrenal chromaffin cells (Tachikawa et al., 2001), and 8-fold higher than that for Rg_3 -induced inhibition in $[\text{Ca}^{2+}]_i$ increase by NMDA treatment in rat hippocampal neurons (Kim et al., 2001). These discrepancies in IC_{50} values might reflect the differential affinity of Rg_3 for ion channels or receptors, suggesting that NMDA or nicotinic acetylcholine receptors might be more sensitive than Na^+ channels to low concentrations of Rg_3 .

The effects of Rg_3 on the activation and inactivation of $\text{Na}_v1.2$. We next examined the effects of Rg_3 on the voltage-dependence of Na^+ channel steady-state activation and inactivation. First, the effect of Rg_3 on Na^+ channel activation was determined by a conductance transformation of the peak current-voltage relationship (Fig. 3A and B), with the curves representing the best data fit using the Boltzmann function. There was a significant depolarizing shift of the half-maximal activation voltage ($V_{g0.5}$). The $V_{g0.5}$ was $-28.9 \pm 0.57 \text{ mV}$ in control experiments and $-17.8 \pm 0.21 \text{ mV}$ in Rg_3 -treated oocytes ($P < 0.01$, compared to control, $n = 10$). However, the slope factor (kg) was not significantly different, yielding values of $4.6 \pm 0.5 \text{ mV}$ under control conditions and $4.8 \pm 0.2 \text{ mV}$ after Rg_3 treatment. We then investigated the effect of Rg_3 on voltage-dependent Na^+ channel inactivation by plotting the normalized peak I_{Na} against the conditioning pre-pulse voltage (Fig. 3C and D), and then fitting the data to

the Boltzmann function. There was no significant difference in the half-maximal inactivation voltage ($V_{h0.5}$) and the slope factor (kh) between control and Rg₃ treatment groups; $V_{h0.5}$ was -28.9 ± 0.57 and -26.9 ± 0.68 mV, respectively, and kh was 7.2 ± 0.4 and 8.1 ± 0.68 mV, respectively ($n = 10$). These findings indicate that Rg₃ affects the steady-state activation but not inactivation of the Na⁺ channel.

Use-dependent blockade of Na_v1.2 by Rg₃ and lidocaine. Since Na⁺ channel blockers such as lidocaine and other antiarrhythmic drugs exhibit use-dependent inhibition (Hondegam and Kazung, 1984), we tested whether Rg₃ behaved in the same way, using Rg₃ concentrations shown to induce minimal I_{Na} blockade (10 μ M) and marked I_{Na} blockade (100 μ M) in our initial tonic block experiments. I_{Na} was elicited by 20-ms pulses from -100 to -10 mV for 50 times at 10 Hz. Each peak I_{Na} was normalized to the first pulse peak I_{Na} . Under control conditions, there was a slight reduction in peak I_{Na} , while treatment with 10 and 100 μ M Rg₃ induced use-dependent inhibitions of peak I_{Na} values by 11 ± 1 and $15 \pm 2\%$, respectively ($n = 9$ each; Fig. 4A). Lidocaine (1000 μ M) treatment also induced a use-dependent inhibition of the peak I_{Na} by $35 \pm 2\%$ ($n = 8$ each) (Fig. 4A). Thus, Rg₃ and lidocaine both appear to induce use-dependent inhibitions of I_{Na} .

The effect of Rg₃ on peak I_{Na} at different holding potentials. The effect of Rg₃ on peak I_{Na} at different holding potentials was examined. Diphenylhydantoin (DPH), which is a well-known anticonvulsant that preferentially binds to the inactivated Na⁺ channel (Valenzuela et al., 1996), did not significantly affect the peak I_{Na} evoked at -10 mV from a holding potential of -110 mV ($6 \pm 1\%$ inhibition by 100 μ M, $n = 10$) (Fig. 5A). However, at a more depolarized holding potential of -50 mV, DPH dramatically

reduced the peak I_{Na} ($86 \pm 7\%$ inhibition by $100 \mu\text{M}$, $n = 10$). This indicates that the blockade of peak I_{Na} by DPH is highly sensitive to the membrane potential and that DPH has a much higher affinity to the inactivated state than to the resting state of the Na^+ channel as shown by Kuo and Bean (1994) (Fig. 5A and C, *left panel*). We then tested the effect of Rg_3 on the peak I_{Na} at different holding potentials. In contrast to the action of DPH, the inhibitory effect of $100 \mu\text{M}$ Rg_3 was not significantly affected by changes in the holding potential ($78 \pm 14\%$ and $69 \pm 10\%$ inhibition at -110 and -50 mV, respectively; $n = 15$ each), indicating that the inhibitory effect of Rg_3 on the peak I_{Na} is independent of the membrane holding potential (Fig. 5B and C, *right panel*).

Lidocaine and tetrodotoxin (TTX) do not prevent Rg_3 -induced inhibition of peak I_{Na} . We performed occlusion experiments using lidocaine and TTX, which are well-known Na^+ channel blockers, to determine whether Rg_3 shares a common binding site or pathway with lidocaine or TTX. As shown in Figures 6B and D, single applications of $30 \mu\text{M}$ Rg_3 , $1000 \mu\text{M}$ lidocaine and 1 nM TTX inhibited the peak I_{Na} values by 42 ± 8 , 25 ± 5 , and $44 \pm 3\%$, respectively. Co-treatment of Rg_3 with lidocaine produced an additive inhibition of peak I_{Na} by $88 \pm 4\%$, while co-treatment of Rg_3 with TTX produced an additive inhibition of peak I_{Na} by $80 \pm 4\%$. These results suggest that Rg_3 regulates Na^+ channels by acting on different site(s) from those of lidocaine and TTX.

The effect of Rg_3 on mutant Na^+ channels. To gain insight into the mechanism(s) by which Rg_3 inhibits peak I_{Na} , we examined the requirement of different Na^+ channel α subunit protein domains using site-directed mutagenesis. We constructed the following six mutant types: 1) mutation of the channel pore entrance of the S6 segment of domain I by replacement of residue Y401 with cysteine (Y401C) or

threonine (Y401T); 2) mutation at the channel pore sites by replacement of E942 with glutamine (E942Q), E945 with glutamine (E945Q) or D927 with asparagine (D927N) (Kontis and Goldin, 1993); 3) mutation of the lidocaine binding sites by replacement of residues F1764 and/or Y1771 with alanine (F1764A or Y1771A and F1764A-Y1771A, respectively) (Ragsdale et al., 1994; 1996); 4) mutation of the extracellular and intracellular TTX binding sites by replacement of F385 with cysteine (F385C), serine (F385S), tyrosine (F385Y) or methionine (F385M), or replacement F387 with glycine (F387G), threonine (F387T) or glutamine (F387Q) (Noda et al., 1989; Terlau et al., 1991); 5) mutation of the S4 voltage-sensor segments of domains I to IV by replacement of residues K226, K859, R1312, or R1638 with glutamine (K226Q, K859Q, R1312Q, or R1638Q) (Kontis et al., 1997); and 6) creation of a fast inactivation gating-deficient mutant by replacing residues IFM with three glutamines (IFMQ3) (West et al., 1992). Representative traces were obtained from oocytes expressing channel pore, TTX binding site, and voltage-sensor mutants in the absence or presence of Rg₃ (Fig. 7A). Rg₃ treatment induced tonic inhibition of the peak I_{Na} in all mutants (Fig. 7 and Table 1). The concentration-response relationship for peak I_{Na} inhibition by Rg₃ in the different kinds of mutants was determined (Fig. 7B), and the data were fitted using the Hill equation. The Hill coefficients and V_{max} values for the mutants were not significantly different from those of the wild-type channels. However, the IC₅₀ values from mutants F385M, E387Q, Y401C and K859Q were significantly higher than that of the wild-type channel ($P < 0.01$, compared to wild-type channel) (Table 1). Since mutations of F1764 or Y1771 to alanine (F1764A or Y1771A) are resistant to lidocaine-induced tonic and use-dependent blockades (Ragsdale et al., 1994; 1996), we examined whether these mutations could affect the Rg₃-mediated tonic and use-dependent inhibitions of peak I_{Na} .

While lidocaine treatment induced only a slight inhibition of peak I_{Na} in oocytes expressing the F1764A, Y1771A and F1764A-Y1771A mutants following low- and high-frequency stimulations (Fig. 8A, C, and E, low-frequency stimulations; Fig. 8B, D, and F, high-frequency stimulations), Rg₃ treatment induced wild-type inhibition levels of peak I_{Na} in the mutants following in both low- and high-frequency stimulations (Fig. 8). The IFMQ3 mutant, which lacks fast inactivation, showed a slower decay and a sizable persistent non-inactivating or plateau current at the end of a 500 ms depolarizing pulse to -10 mV in the absence of Rg₃, which is consistent with a previous report (West et al., 1992). In the IFMQ3 mutant, Rg₃ treatment induced dose-dependent inhibitions of peak and plateau I_{Na} (Fig. 9A). The plateau I_{Na} showed a larger change; the IC₅₀ values of Rg₃ acting on the on peak and plateau I_{Na} in this mutant were 38 ± 3 and 14 ± 4 μ M, respectively (approximately a three-fold difference). These results suggest that Rg₃ interacts more readily with the open state of the Na⁺ channel versus the resting state (Fig. 9B). Finally, we examined whether the IFMQ3 mutant showed any changes in the inhibitory effect of Rg₃ on oocytes subjected to high-frequency stimulation. We observed that Rg₃ treatment induced a two- to three-fold larger use-dependent inhibition in IFMQ3 mutant channels versus wild-type channels; 10 and 100 μ M Rg₃ induced 17 ± 1 and $45 \pm 4\%$ use-dependent inhibitions of I_{Na} , respectively ($n = 11$) (Fig. 4A and B). In contrast, Rg₃ did not induce additional use-dependent inhibitions in the other tested mutants (data not shown). Collectively, these results further demonstrate that Rg₃ uses different binding site(s) from those of lidocaine and TTX and that Rg₃ blocks the resting and open state of brain Na⁺ channels.

A point mutation in the S4 voltage-sensor segment of domain II of Nav1.2 abolishes the Rg₃-induced voltage shift of Na⁺ channel activation. As shown in

Figures 3A and B, Rg₃ treatment strongly depolarized the Na⁺ channel activation voltage, suggesting that Rg₃ might modify its activation gating. The S4 segments comprise four homologous domains (I-IV) of the Na⁺ channel, and are believed to act as the voltage-sensing apparatus (Kontis et al., 1997). To investigate whether mutations in the voltage-sensor segments of the Na⁺ channel affect the Rg₃-induced depolarization of the Na⁺ channel activation voltage, we constructed four different mutants in the S4 segments of domain I to IV (Table 1) (Kontis et al., 1997), and examined their influences on the Rg₃-induced voltage shift of the Na⁺ channel activation curve. Our results revealed that replacing K859 (domain II) with glutamine (K859Q) abolished the Rg₃-induced voltage shift, although the mutation itself resulted in a depolarizing shift of the activation curve by ~ 10 mV compared to wild-type channel (Fig. 3C and D). The half-maximal activation voltage ($V_{g0.5}$) was -10.9 ± 0.4 mV and the slope factor (k_g) was 5.1 ± 0.3 mV in the Rg₃ control, but only -9.8 ± 0.4 mV and 5.3 ± 0.4 mV in the mutant (Fig. 3C and D). The other tested mutants did not show significant alterations of the activation curve (data not shown), indicating that the K859 residue of domain II may play an important role in the Rg₃-induced modification of voltage-dependent Na⁺ channel activation.

A single point mutation in the S4 voltage-sensor segment of domain II of Na_v1.2 in both wild-type and IFMQ3 mutant channels abolishes Rg₃-induced use-dependent inhibition. We next examined whether the K859Q mutation affects the Rg₃-induced use-dependent inhibition of Na⁺ channels, since this mutation abolished Rg₃-induced modification of Na⁺ channel activation gating. Rg₃ treatment did not produce use-dependent inhibition in either K859Q or IFMQ3-K859Q mutants (Fig. 4C and D), suggesting that the K859 residue of the S4 voltage sensor segment of domain II might

play an important role in Rg₃-induced use-dependent inhibition of the IFMQ3 mutant. These mutations also significantly increased the IC₅₀ values by 1.5-fold compared to wild-type in terms of tonic inhibition ($^*P < 0.01$, compared to wild-type, Table 1). Interestingly, lidocaine treatment produced wild-type level use-dependent inhibition in the K859Q mutant (Fig. 4C), suggesting that the Rg₃ site is not related with the action of lidocaine. In contrast, when we examined whether the mutation in the S4 voltage-sensor segment of domain II affected Rg₃-induced open-channel blocking pattern, we found that Rg₃ treatment inhibited both peak and plateau I_{Na} levels to comparable degrees in the IFMQ3-K859Q and IFMQ3 mutants (compare Fig. 9C and A). The IC₅₀ values of the IFMQ3-K859Q mutant were 56 ± 6 and 20 ± 1 μ M for the peak and plateau I_{Na} levels, respectively (Fig. 9D and Table 1), which was significantly higher than that for the IFMQ3 mutant in terms of peak (1.5-fold) but not plateau I_{Na} inhibition ($^{**}P < 0.01$, compared to IFMQ3 mutant, Table 1). These results indicate that the K859Q mutant might decrease the affinity of Rg₃ for the IFMQ3 mutant to a comparable degree as that seen in the wild-type, but that the K859Q mutation did not affect the Rg₃-induced open channel blocking pattern.

Developmental rate of Rg₃-induced open channel blockade. We examined the ability of various concentrations of Rg₃ to block IFMQ3 (Fig. 10A). Untreated control traces showed that during a depolarizing pulse to -10 mV, the IFMQ3 current decayed exponentially with a single, slow time constant (τ_{slow}) of 585.4 ± 2.7 ms ($n = 9$). Currents elicited after Rg₃ treatment decayed exponentially with two distinct time constants. In the presence of low concentration of Rg₃ like 10 μ M the currents decayed with a slow time constant that was similar to that of the control, while treatment with higher concentrations of Rg₃ such as 30 to 300 μ M induced a concentration-dependent

fast exponential component to the curves (τ_{fast}), which represented the Rg₃ block (τ_{B}). The time constants of the fast components were 464.5 ± 6.4 , 235.1 ± 7.8 , 64.1 ± 14.2 and 51.8 ± 9.4 ms in samples treated with 10, 30, 100 and 300 μM Rg₃, respectively. This result indicates that Rg₃ also interacts with the open state of the Na⁺ channel. A plot of the reciprocal of τ_{B} ($1/\tau_{\text{B}}$) against drug concentration (Lansman et al., 1986) was used to approximate the drug-channel interaction kinetics. The relationship between $1/\tau_{\text{B}}$ and the concentration of Rg₃ was determined with a straight line representing the best fit to the equation $1/\tau_{\text{B}} = k_{\text{on}}[\text{Rg}_3] + l$. (Fig. 10B). The slope of the line is the apparent binding constant (k_{on}), which equals $0.062 \pm 0.009 \times 10^6 \text{M}^{-1}\text{s}^{-1}$, and the intercept l equals $1.89 \pm 0.78 \text{s}^{-1}$. The latter value is close to the reciprocal of τ_{slow} ($1.71 \pm 0.41 \text{s}^{-1}$), indicating that in the IFMQ3 mutant, a residual inactivation determines the intercept in the absence of Rg₃. This suggests that the unbinding constant (k_{off}) is likely to be very small.

Rg₃ treatment slows recovery from inactivation. Since Rg₃ blocked the open state of the IFMQ3 channel (Fig. 9) and exhibited an additional use-dependent block compared to the wild-type channel (Fig. 4B), we lastly examined whether the inhibitory effect of Rg₃ on I_{Na} was derived from a delayed recovery of the channel from the open channel block. Current traces were recorded in the absence (Fig. 10C, control, upper panel) and presence (Fig. 10C, lower panel) of 100 μM Rg₃ with a recovery time interval of 10 ms between pulses. Recovery from open channel block was analyzed as shown in Figure 10D. After a 10-ms pre-pulse (P1), recovery from open channel block was assessed using a test pulse (P2) after increasing recovery intervals (Fig. 10C and D, *inset*). The IFMQ3 Na⁺ channels were found to recover rapidly, likely due to a slow inactivation associated with the mutation (< 50 ms, closed circles, Fig. 10D). In contrast,

Rg₃ treated channels (open circles, Fig. 10D) showed a delayed recovery from open channel block (up to 260 ms). This slow recovery appears to underlie the enhanced use-dependent inhibition produced by Rg₃.

Discussion

Ginseng has long been used as a treatment for a wide variety of ailments, and some of the purported effects of this root have been documented in laboratory studies (Nah, 1997). Although the beneficial effects and functional mechanisms of ginsenosides have not been fully elucidated, accumulating evidence suggest that they may target the ion channels involved in neuronal excitability. Ginsenosides have been shown to affect several ion channels found at pre- and post-synaptic sites in the nervous system (Choi et al., 2002; 2003; Sala et al., 2002; Nah and McCleskey, 1994; Nah et al., 1995; Kim et al., 1998; Kim et al., 2002), and their effects are closely coupled to the inhibition of neurotransmitter release (Kudo et al., 1998; Tachikawa et al., 1995). We recently demonstrated that Rg₃ stereospecifically inhibits voltage-dependent brain Na⁺ currents, and that the carbohydrate portion of Rg₃ plays a key role in the inhibition of Na⁺ currents (Kim et al., 2005). However, very little is known about the molecular mechanism(s) underlying Rg₃-induced Na⁺ channel modulation.

Here, we characterized Rg₃-induced channel regulation of brain Na⁺ channels (Nav1.2) expressed in *Xenopus* oocytes. Our results revealed four major findings. First, Rg₃ produced a tonic inhibition of the peak I_{Na} via an interaction with the resting state of the Na⁺ channel (Fig. 2). Second, Rg₃ induced a large depolarizing shift in the steady-state activation of the Na⁺ channel (Fig. 3). Third, Rg₃ produced a use-dependent block of the Na⁺ channel following high-frequency stimulation, indicating that Rg₃ could exert

an inhibitory effect on the open state of the Na^+ channel (Fig. 4). And fourth, the inhibitory effect of Rg_3 on the peak I_{Na} was independent of the holding potential, indicating that Rg_3 might have a lower affinity for the inactivated state of the Na^+ channel (Fig. 5).

To examine the molecular mechanism by which Rg_3 regulates brain Na^+ channel activity, we used site-directed mutagenic methods similar to those previously used to identify drug- or toxin- Na^+ channel interaction site(s) (Cestele and Catterall, 2000). We utilized six different types of $\text{Na}_v1.2$ mutants to assess the sites at which Rg_3 interacts with Na^+ channels: 1) mutations in the channel pore entrance of the S6 segment of domain I; 2) mutations in the pore region of domain II; 3) mutations in the lidocaine binding sites; 4) mutations in the TTX binding sites; 5) mutations in the S4 voltage-sensor segments of domains I, II, III and IV; and 6) mutations in the inactivation cluster. The pore site(s) are unlikely to be the target for Rg_3 , since the inhibitory potency of Rg_3 on Na^+ channel activity was not altered in cells injected with pore site mutants (Fig. 7 and Table 1). In addition, it does not appear as though Rg_3 interacts with the binding sites for lidocaine or TTX (Ragsdale et al., 1994; 1996), since the inhibitory potency of Rg_3 on Na^+ channel activity was not altered in cells injected with the F385C, F385S, F385Y, F385T, F385M, E387G, E387T, E387Q, F1764A, Y1771A or F1764A-Y1771A mutants, which harbor changes in the lidocaine or TTX binding sites (Fig. 7 and Table 1). In addition, the inhibitory effect of Rg_3 on the peak I_{Na} appeared additive in the presence of lidocaine or TTX in occlusion experiments (Fig. 6C and D), providing further evidence that Rg_3 utilizes a separate binding site. Finally, we tested the possibility that the hydrophobic cluster related with Na^+ channel inactivation might be involved in the Rg_3 -induced inhibition of I_{Na} . In the IFMQ3 mutant channel, which

lacks fast inactivation (West, 1992), Rg₃ treatment inhibited the non-inactivating plateau I_{Na} to a greater degree than the peak I_{Na} , providing further evidences that Rg₃ inhibits I_{Na} in both the open and resting states of the Na⁺ channel.

Two other lines of evidence supporting the possibility that Rg₃ also inhibits open Na⁺ channels are the observation that 1) the inhibitory effect of Rg₃ on peak I_{Na} is not dependent on membrane holding potentials, and 2) that Rg₃ does not shift the steady-state inactivation curve in wild-type Na⁺ channels (Figs. 3 and 5), which does occur in many drugs (e.g. anti-arrhythmic agents and anticonvulsants) that act on inactivated Na⁺ channels (Willow et al., 1985). Moreover, Rg₃ treatment induced an additional use-dependent block of I_{Na} in the IFMQ3 mutant compared to wild-type channel, indicating that Rg₃ might prefer to bind and block the open state of the Na⁺ channel. Similar use-dependent open channel blockades have been observed in the case of disopyramide, RSD921, tetracaine and flecainide (Cahalan, 1978; Grant et al., 1996; Pugsley and Goldin, 1999; Ramos and O'Leary, 2004; Wang et al, 2003).

We next used S4 voltage-sensor segment mutants (K226Q, K859Q, R1312Q and R1368Q) to examine whether the voltage-sensor segment of the Na⁺ channel was involved in Rg₃-induced Na⁺ channel regulation (Noda et al., 1989). The K859Q mutation in domain II, but not K226Q, R1312Q or R1638Q, significantly increased the IC₅₀ values by 1.5-fold compared to wild-type ($^*P < 0.01$, compared to wild-type, Table 1), indicating that this mutation might decrease the affinity of Rg₃ to Na⁺ channels. In addition, K859Q alone abolished the Rg₃-induced voltage shift in Na⁺ channel activation (Fig. 3C), and Rg₃-induced use-dependent but not tonic inhibition of I_{Na} (Figs. 4C and Fig. 7). Although these results do not allow precise elucidation of the interaction between Rg₃ and Na⁺ channels, our data seem to indicate that the voltage-sensor S4

segment of domain II might be an important portion for Rg₃-induced Na⁺ channel regulation (Figs. 3C and 4C). It is unlikely that Rg₃ interacts non-specifically with Na⁺ channels, since the 20(*S*)-ginsenoside Rg₃ used in the present study inhibits *I*_{Na}, but 20(*R*)-ginsenoside Rg₃ does not (Jeong et al., 2004) (Fig. 1). Moreover, modifications of the hydrophilic portion of Rg₃ by opening the cyclic glucoses or conjugating the glucoses with other hydrophobic molecule abolished the inhibitory effect of Rg₃ on peak *I*_{Na} (Kim et al., 2005). These findings indicate that Rg₃ specifically modulates Na⁺ channel by interaction with unidentified site of Na⁺ channel. Further works will be necessary to determine specific interaction site(s) of Rg₃ with Na⁺ channel.

Based on our findings, it seems reasonable to speculate as to whether the *in vitro* Rg₃-induced Na⁺ channel blockade could translate to *in vivo* pharmacological effects. Qian et al. (2005) and Xie et al. (2005) determined plasma concentration of Rg₃ after administration of Rg₃ via intravenous (5 mg/kg) or intragastric (10 mg/kg) routes in rats, and found that plasma Rg₃ peaked at 1 µg/ml 10 min after intravenous administration and 4 h after intragastric administration. These findings suggest that plasma-borne Rg₃ might exert *in vivo* pharmacological effects. Also in rats, Bae et al. (2004) and Tian et al. (2005) showed that oral (100 mg/kg) or intravenous administration (5 and 10 mg/kg) of Rg₃ exerted significant neuroprotective effects against focal cerebral ischemic injury by decreasing neurological deficit scores and reducing the infarct area compared with the control group. Rg₃ also significantly improved mitochondrial energy metabolism, antagonized decreases in superoxide dismutase and glutathione-peroxidase activities, and increased malondialdehyde levels in a cerebral ischemia model (Tian et al., 2005). Na⁺ channel blocking drugs such as local anesthetics, antiarrhythmics and anticonvulsants have been shown to exhibit significant neuroprotective effects against

cerebral ischemia-, hypoxia- and head trauma-induced neuronal damages (Taylor and Meldrum, 1995). Thus, it is possible that Rg₃-mediated brain I_{Na} inhibition could be an underlying mechanism for neuroprotection against *in vivo* ischemic brain injury.

We previously demonstrated that Rg₃ and other ginsenosides inhibit voltage-dependent Ca²⁺ and K⁺ channels as well as ligand-gated ion channels such as 5-HT₃ and some subsets of nicotinic acetylcholine receptors (Choi et al., 2002; Choi et al., 2003; Jeong et al., 2005; Nah et al., 1995). We are currently examining the detailed characteristics of Rg₃-mediated regulation of Ca²⁺, K⁺ and ligand-gated ion channels. The elucidation of the regulatory modes and identification of interaction site(s) with those channels or receptors by Rg₃ and other ginsenosides will provide important insights into the molecular basis by which ginsenosides interact with membrane proteins such as ion channels and receptors.

Here, we used brain Na⁺ channel gene expression in a *Xenopus* oocyte model system to show that Rg₃ blocks the resting and open state of brain Na⁺ channels. This novel work provides new insights into one possible mechanism underlying the effects of ginsenosides in the nervous system.

References

- Bae EA, Hyun YJ, Choo MK, Oh JK, Ryu JH, and Kim DH (2004) Protective effect of fermented red ginseng on a transient focal ischemic rats. *Arch Pharm Res.* **27**:1136-1140.
- Bean BP, Cohen CJ, and Tsien RW (1983) Lidocaine block of cardiac sodium channels. *J. Gen. Physiol.* **81**:613-642.
- Cahalan MD (1978) Local anesthetic block of sodium channels in normal and pronase-treated squid giant axons. *Biophys. J.* **23**:285-311.
- Catterall WA (1987) Identification of an alpha subunit of dihydropyridine-sensitive brain calcium channels. *Trends in Pharmacol. Sci.* **8**:57-65.
- Cestele S, and Catterall WA (2000) Molecular mechanisms of neurotoxin action on voltage-gated sodium channels. *Biochimie* **82**:883-892.
- Choi S, Jung SY, Lee JH, Sala F, Criado M, Mulet J, Valor LM, Sala S, Engel AG., and Nah SY (2002) Effects of ginsenosides, active components of ginseng, on nicotinic acetylcholine receptors expressed in *Xenopus* oocytes. *Eur. J. Pharmacol.* **442**:37-45.
- Choi S, Lee JH, Oh S, Rhim H, Lee SM, and Nah SY (2003) Effects of ginsenoside Rg₂ on the 5-HT_{3A} receptor-mediated ion current in *Xenopus* oocytes. *Mol. Cells* **15**: 108-113.
- Dascal N (1987) The use of *Xenopus* oocytes for the study of ion channels. *CRC Crit Rev Biochem* **22**:317-387.
- Goldin AL (1995) Voltage-gated Na⁺ channels. In: North, R. A. (Ed.), Ligand- and voltage-gated ion channels, CRC Press, Boca Raton, FL, p. 73-89.

- Grant AO, John JE, Nesterenko VV, Starmer CF, and Moorman JR (1996) The role of inactivation in open-channel block of the sodium channel: studies with inactivation-deficient mutant channels. *Mol. Pharmacol.* **50**:1643-1650.
- Hodgkin AL, and Huxley AF (1952) A quantitative description of membrane current and its application to conduction and excitation in nerve. *J Physiol. (London)* **117**:500-544.
- Hondegham LM, and Kazung BG. (1984) Antiarrhythmic Agents: The Modulated Receptor Mechanism of Action of Sodium and Calcium Channel-Blocking Drugs *Annu. Rev. Pharmacol. Toxicol.* **24**:387-423.
- Jeong SM, Lee JH, Kim JH, Lee BH, Yoon IS, Lee JH, Kim DH, Rhim H, Kim Y, and Nah SY (2004) Stereospecificity of ginsenoside Rg₃ action on ion channels. *Mol. Cells* **18**:383-389.
- Kim HS, Lee JH, Goo YS, and Nah SY (1998) Effects of ginsenosides on Ca²⁺ channels and membrane capacitance in rat adrenal chromaffin cells. *Brain Res. Bull.* **46**:245-251.
- Kim JH, Hong YH, Lee JH, Kim DH, Jeong SM, Lee BH, Lee SM, and Nah SY (2005) A role for the carbohydrate portion of ginsenoside Rg₃ in Na⁺ channel inhibition. *Mol. Cells* **19**:137-142.
- Kim S, Ahn K, Oh TH, Nah SY, and Rhim H (2002) Inhibitory effect of ginsenosides on NMDA receptor-mediated signals in rat hippocampal neurons. *Biochem. Biophysical. Res. Comm.* **296**:247-254.
- Kontis KJ, and Goldin AL (1993) Site-directed mutagenesis of the putative pore region of the rat IIA sodium channel. *Mol. Pharmacol.* **43**:635-644.
- Kontis KJ, Rounaghi R, and Goldin AL (1997) Sodium channel activation gating is

- affected by substitutions of voltage sensor positive charges in all four domains. *J. Gen. Physiol.* **110**:391-401.
- Kudo K, Tachikawa E, Kashimoto T, and Takahashi E (1998) Properties of ginseng saponin inhibition of catecholamine secretion in bovine adrenal chromaffin cells. *Eur. J. Pharmacol.* **341**:139-144.
- Kuo CC, and Bean BP (1994) Slow binding of phenytoin to inactivated sodium channels in rat hippocampal neurons. *Mol. Pharmacol.* **46**:716-725.
- Kuo CC, Chen RS, Lu L, and Chen RC (1997) Carbamazepine inhibition of neuronal Na⁺ currents: quantitative distinction from phenytoin and possible therapeutic implications. *Mol. Pharmacol.* **51**:1077-1083.
- Lansman JB, Hess P, and Tsien RW (1986) Blockade of current through single calcium channels by Cd²⁺, Mg²⁺, and Ca²⁺. Voltage and concentration dependence of calcium entry into the pore. *J. Gen. Physiol.* **88**:321-347.
- Nah SY, and McCleskey EW (1994) Ginseng root extract inhibits calcium channels in rat sensory neurons through a similar path, but different receptor, as μ -type opioids. *J. Ethnopharmacol.* **42**:45-51.
- Nah SY, Park HJ, and McCleskey EW (1995) A trace component of ginseng that inhibits Ca²⁺ channels through a pertussis toxin-sensitive G protein. *Proc. Natl. Acad. Sci. USA* **92**:8739-8743.
- Nah SY (1997) Ginseng, recent advances and trend. *Korea J. Ginseng Sci.* **21**:1-12.
- Noda M, Suzuki H, Numa S, and Stühmer W (1989) A single point mutation confers tetrodotoxin and saxitoxin insensitivity on the sodium channel II. *FEBS Lett.* **259**: 213-216
- Pugsley MK, and Goldin AL (1998) Effects of bisaramil, a novel class I antiarrhythmic

- agent, on heart, skeletal muscle and brain Na⁺ channels. *Eur. J. Pharmacol.* **343**:93-104.
- Pugsley MK, and Goldin AL (1999) Molecular analysis of the Na⁺ channel blocking actions of the novel class I anti-arrhythmic agent RSD 921. *Br. J. Pharmacol.* **127**:9-18.
- Pugsley MK, Yu EJ, and Goldin AL (2000) Spiradoline, a kappa opioid receptor agonist, produces tonic- and use-dependent block of sodium channels expressed in *Xenopus* oocytes. *Gen. Pharmacol.* **34**:417-427.
- Qian T, Cai Z, Wong RN, Mak NK, and Jiang ZH (2005) In vivo rat metabolism and pharmacokinetic studies of ginsenoside Rg₃. *J. Chromatogr. B.* **816**:223-32.
- Ragsdale DS, McPhee JC, Scheuer T, Catterall WA (1994) Molecular determinants of state-dependent block of Na⁺ channels by local anesthetics. *Science* **265**:1724-1728.
- Ragsdale DS, McPhee JC, Scheuer T, Catterall WA (1996) Common molecular determinants of local anesthetic, antiarrhythmic, and anticonvulsant block of voltage-gated Na⁺ channels. *Proc. Natl. Acad. Sci. USA* **93**:9270-9275.
- Ramos E and O'Leary ME (2004) State-dependent trapping of flecainide in the cardiac sodium channel. *J. Physiol.* **560**:37-49.
- Sala F, Mulet J, Choi S, Jung SY, Nah SY, Rhim H, Valor LM, Criado M, and Sala S (2002) Effects of ginsenoside Rg₂ on human neuronal nicotinic acetylcholine receptors. *J. Pharmacol. Exp. Ther.* **301**:1052-1059.
- Stuart GJ, and Sakmann B (1994) Active propagation of somatic action potentials into neocortical pyramidal cell dendrites. *Nature* **367**:60-72.
- Tachikawa E, Kudo K, Kashimoto, T, and Takahashi E (1995) Ginseng saponins reduce acetylcholine-evoked Na⁺ influx and catecholamine secretion in bovine adrenal

- chromaffin cells. *J. Pharm. Exp. Ther.*, **273**:629-636.
- Talyor CP, and Meldrum BS (1995) Na⁺ channels as targets for neuroprotective drugs. *Trends Pharmacol.* **16**:309-316.
- Terlau H, Heinemann SH, Stühmer W, Pusch M, Conti F, Imoto K, and Numa S (1991) Mapping the site of block by tetrodotoxin and saxitoxin of sodium channel II. *FEBS Lett.* **293**:93-96.
- Tian J, Fu F, Geng M, Jiang Y, Yang J, Jiang W, Wang C, and Liu K (2005) Neuroprotective effect of 20(S)-ginsenoside Rg₃ on cerebral ischemia in rats. *Neurosci Lett.* **374**:92-97.
- Valenzuela C, Delpon E, Franqueza L, Gay P, Perez O, Tamargo J, and Snyders DJ (1996) Class III antiarrhythmic effects of zatebradine. Time-, state-, use-, and voltage-dependent block of hKv1.5 channels. *Circ.* **94**:562-570.
- Wang GK, Russell C, and Wang SY (2003) State-dependent block of wild-type and inactivation-deficient Na⁺ channels by flecainide. *J. Gen. Physiol.* **122**:365-374.
- Wang SH, and Wang GK (2003) Voltage-gated sodium channels as primary targets of diverse lipid-soluble neurotoxins. *Cellular Signalling* **15**:151-159.
- West JW, Patton DE, Scheuer T, Wang Y, Goldin AL, and Catterall WA (1992) A cluster of hydrophobic amino acid residues required for fast Na⁺ channel inactivation. *Proc. Natl. Acad. Sci. USA* **89**:10910-10914.
- Willow M, Gono T, and Catterall WA (1985) Voltage clamp analysis of the inhibitory actions of diphenylhydantoin and carbamazepine on voltage-sensitive sodium channels in neuroblastoma cells. *Mol. Pharmacol.* **27**:549-558
- Xie HT, Wang GJ, Sun JG, Tucker I, Zhao XC, Xie YY, Li H, Jiang XL, Wang R, Xu MJ and Wang W (2005) High performance liquid chromatographic-mass

spectrometric determination of ginsenoside Rg₃ and its metabolites in rat plasma using solid-phase extraction for pharmacokinetic studies. *J. Chromatogr. B.* **818**:167-173.

Footnotes

This work was supported in part by a grant from the Korean Food Research Institute (2004), the Neurobiology Research Program from the Korean Ministry of Science and Technology (to S. Y. Nah), and two Brain Research Center of the 21st Century Frontier Research Program grants funded by the Korea Ministry of Science and Technology (M103KV010008-05K2201-00830 and M103KV010004-03K2201-00420).

Legends for Figures

Fig. 1. Structure of the 20(S)-ginsenoside Rg₃ (Rg₃). Glc, glucopyranoside. Subscripts indicate the carbon in the glucose ring that links the two carbohydrates.

Fig. 2. Tonic inhibition of I_{Na} by Rg₃ and lidocaine. A, Oocytes were injected with wild-type Na_v1.2 α and β 1 subunit cRNAs and maintained for 2-4 days before Na⁺ currents (I_{Na}) were recorded in ND96 using the two-electrode voltage clamp technique. Open circles represent the peak inward current amplitudes elicited by 100 ms depolarizations to -10 mV from a holding potential of -100 mV, evoked every 5 s. Rg₃ (100 μ M) or lidocaine (1000 μ M) were applied during the period indicated by the solid bars. *Inset left*, traces are representatives of six separate oocytes from three different frogs. *Inset right*, the histograms show the percent blockade of peak I_{Na} by Rg₃ or lidocaine (Lido).

Data represent the means \pm S.E.M. ($n = 10-13/\text{group}$). *B*, The current-voltage relationship was obtained using voltage steps between -50 and $+50$ mV taken in 5 mV increments. Voltage steps were applied in the absence (\bullet) and presence (\circ) of $100 \mu\text{M}$ Rg_3 or after washout of Rg_3 (\blacktriangledown). Data represent the means \pm S.E.M. ($n = 5-6/\text{group}$). *C* and *D*, Concentration-response curves for the Rg_3 (*C*) or lidocaine (*D*) -induced inhibition of peak I_{Na} . *Inset*, traces are representatives of six separate oocytes from three different frogs. The solid lines were fit by the Hill equation as described in the Experimental Procedures. Data represent the means \pm S.E.M. ($n = 10-13/\text{group}$).

Fig. 3. The effect of Rg_3 on steady-state activation and inactivation of I_{Na} in wild-type and K859Q mutant channels. *A*, Effect of Rg_3 on steady-state activation and inactivation of I_{Na} in wild-type channels. The voltage-dependence of conductance was compared in the absence (\bullet) and presence (\circ) of $100 \mu\text{M}$ Rg_3 . Inactivation was measured using a two-pulse protocol in which oocytes were held at -100 mV and depolarized to potentials from -60 to $+20$ mV for 200 ms, followed by a test-pulse to -10 mV for 10 ms to determine channel availability. Inactivation curves are shown in the absence (\blacksquare) and presence of $100 \mu\text{M}$ Rg_3 (\square). *B*, Representative current traces for the activation and inactivation of wild-type channels were obtained as described in the Experimental Procedures. The indicated traces are presented for clarity. *C*, The effect of Rg_3 on the steady-state activation and inactivation of I_{Na} in the K859Q mutant. *D*, Representative current traces for the activation and inactivation of the K859Q mutant channel were obtained as described. The indicated traces are represented for clarity. Data represent the means \pm S.E.M. ($n = 10-11/\text{group}$). The curves represent a two-state Boltzmann function.

Fig. 4. Use-dependent block of Na^+ channels by Rg_3 or lidocaine. Fifty 20 ms depolarizing pulses to -10 mV were applied from a holding potential of -100 mV at 10 Hz in the absence (\bullet) or presence of 10 (\circ) or 100 (\blacktriangledown) μM Rg_3 in wild-type (A), IFMQ3 (B), K859Q (C) and IFMQ3-K859Q (D) mutants. Lidocaine (1000 μM) (\square) was also applied in wild-type (A) and the K859Q mutant (C). The current amplitude during each pulse was normalized to the peak current of the first pulse and plotted as a function of the pulse number. *Inset*, only sweeps 1 and 50 are shown for both control and Rg_3 treatment groups in the wild-type and mutants (IFMQ3, K859Q and IFMQ3-K859Q). The other sweeps were omitted for clarity. Data represent the means \pm S.E.M. ($n = 9$ -10/group).

Fig. 5. Rg_3 -induced I_{Na} inhibition is independent of the holding potential. A, Representative traces of I_{Na} in the absence or presence of 30 or 100 μM phenytoin (DPH). Each oocyte was held at -50 or -100 mV and stepped to -10 mV for 100 ms every 5 s. B, Representative traces of I_{Na} in control oocytes or those treated with 30 or 100 μM Rg_3 . Each oocyte was held at -50 or -100 mV and stepped to -10 mV for 100 ms every 5 s. C, *left panel*, histograms for the inhibition of I_{Na} by 30 or 100 μM DPH at different holding potentials. C, *right panel*, histograms for the inhibition of I_{Na} by 30 or 100 μM Rg_3 at different holding potentials. Data represent the means \pm S.E.M. ($n = 10$ -11/group).

Fig. 6. Lidocaine and TTX do not interfere with the action of Rg_3 . A, Open circles

represent peak inward current amplitudes elicited by 100 ms depolarizations to -10 mV from a holding potential of -100 mV, evoked every 5 s. Rg₃ (30 μ M) was first applied during the period indicated by the solid bars, and then lidocaine (1000 μ M) was applied in absence or presence of Rg₃ (30 μ M) as indicated by the solid bars. *B*, Traces are representatives of six separate oocytes from three different frogs. *Inset*, the histograms show the percent blockade of I_{Na} by Rg₃, lidocaine (Lido), or Rg₃ + lidocaine (Lido). Data represent the means \pm S.E.M. ($n = 10$ -13/group). *C and D*, Experiments were performed as above with TTX (1 nM) used in place of lidocaine. Data represent the means \pm S.E.M. ($n = 10$ -12/group).

Fig. 7. Effect of Rg₃ on various mutant Na⁺ channels. The site-directed mutants were generated at the channel pore, the lidocaine or TTX binding sites, and the S4 voltage sensor segment of domains I and II, as described in the Experimental Procedures. *A*, Traces are representative of six separate oocytes from three different frogs for analysis of channels with mutations in the channel pore, TTX-interaction site, and S4 voltage sensor segment of domain II. *B*, Representative concentration-response curves for the effect of Rg₃ on various mutants. The solid lines were fit by the Hill equation. Additional IC₅₀, Hill coefficient, and V_{max} values for the various mutants are presented in Table 1.

Fig. 8. The effect of Rg₃ or lidocaine on F1764A, Y1771A and F1764A-Y1771A mutant Na⁺ channels. The site-directed mutants, F1764A, Y1771A, and F1764A-Y1771A, were constructed as described in the Experimental Procedures. *A*, *C* and *E*, Traces are representatives of six separate oocytes from three different frogs for the F1764A (*A*),

Y1771A (*C*), and F1764A-Y1771A (*E*) mutants, respectively. *B*, *D* and *F*, Rg₃ but not lidocaine inhibited peak I_{Na} in a use-dependent manner in the F1764A (*B*), Y1771A (*D*), and F1764A-Y1771A (*F*) mutants. *Insets*, only sweeps 1 and 50 are shown for control (●), 1000 μ M lidocaine (○), and 100 μ M Rg₃ (▼). The other sweeps were omitted for clarity. Data represent the means \pm S.E.M. ($n = 9-10$ /group).

Fig. 9. The effects of Rg₃ on IFMQ3 mutant Na⁺ channels. The IFMQ3 mutant was constructed as described in the Experimental Procedures. *A*, I_{Na} was elicited in IFMQ3 mutant by a 500 ms depolarization to -10 mV from a holding potential of -100 mV, evoked every 5 s. The evoked current exhibited a slower decay and sizable persistent non-inactivating or plateau current. Rg₃ treatment dose-dependently inhibited the peak and plateau I_{Na} values. *B*, Concentration-response curves for the effect of Rg₃ on the IFMQ3 peak (●) and plateau (○) I_{Na} values. The solid lines were fit by the Hill equation. *C*, Current traces of the IFMQ3-K859Q mutant in the absence or presence of Rg₃ were obtained from the procedures described in *A*. *D*, Concentration-response curves for the effect of Rg₃ on IFMQ3-K859Q peak (●) and plateau (○) I_{Na} values. The IC₅₀, Hill coefficient, and V_{max} values for Rg₃ in these mutants are presented in Table 1. Data represent the means \pm S.E.M. ($n = 10-11$ /group).

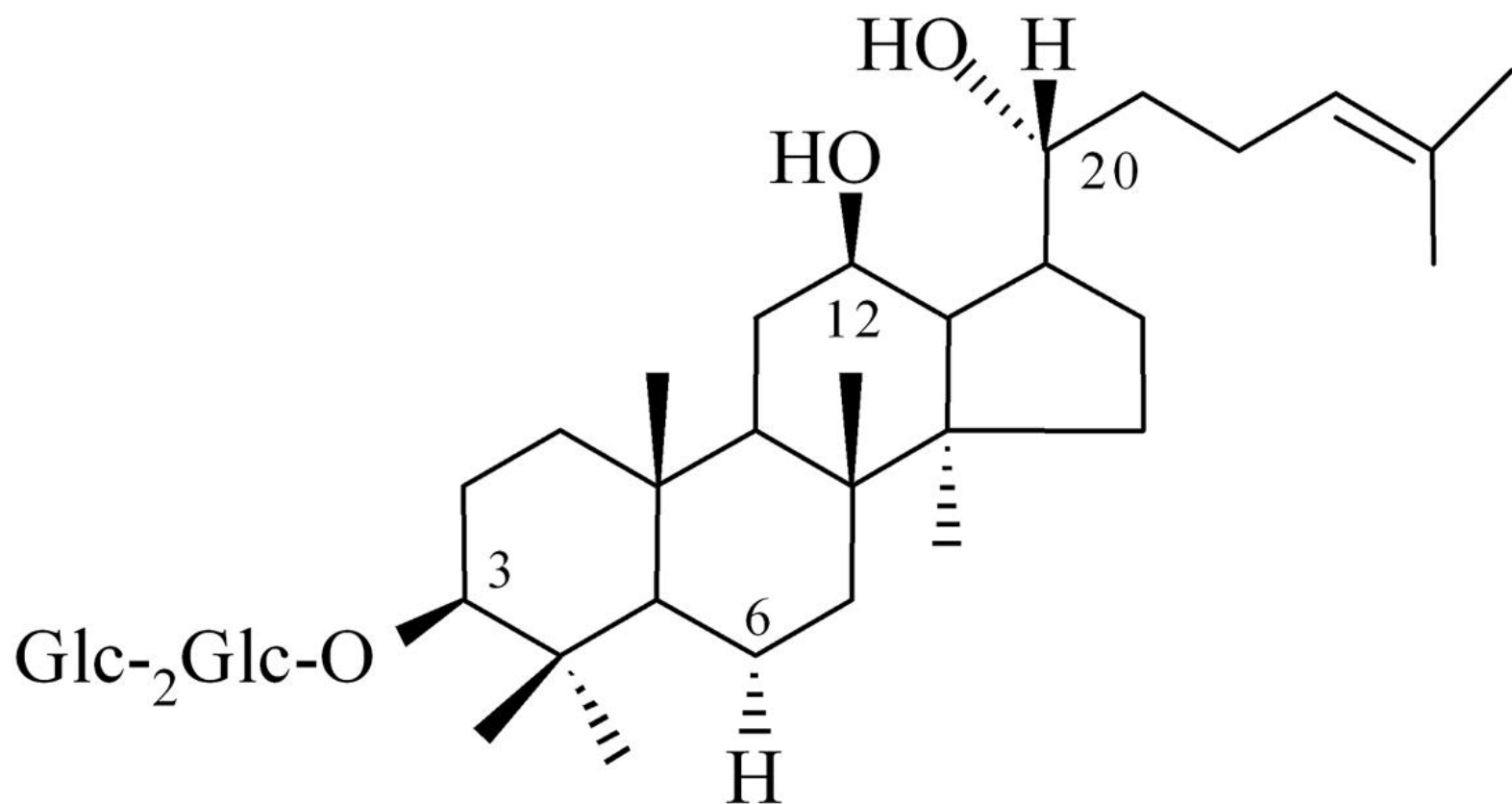
Fig. 10. Kinetics of open channel blockade by Rg₃ and recovery delay in IFMQ3 mutant Na⁺ channels. *A*, Traces evoked from -100 mV to -10 mV in the absence (Con) and presence of various concentrations of Rg₃ showing open channel blockade of IFMQ3. *B*, The rate of Rg₃ block as a function of Rg₃ concentration. A detailed description of the determination of τ_B can be found in the text. Data represent the means \pm S.E.M. ($n = 10-$

12/group). *C*, Delayed recovery of IFMQ3 channels from open channel blockade by Rg₃. Shown is a representative pair of current traces recorded in the absence (Con, *upper*) and presence (Rg₃, *lower*) of 100 μ M Rg₃ with a recovery time interval of 10 ms between pulses. Channels recovered almost fully at this recovery interval in the absence of Rg₃. In the presence of 100 μ M Rg₃, the test current measured during the second pulse (P2) was significantly reduced. *D*, Recovery from inactivation or open channel blockade was assessed in detail using the paired-pulse voltage-clamp protocol shown in the *inset*. After oocytes were depolarized for 10 ms (P1), fractional recovery during a subsequent test pulse (P2) was assessed after an intervening recovery interval. Rg₃ (●)-free channels recovered rapidly (<50 ms), while complete recovery from inactivation was delayed for 260 ms in the presence of Rg₃ (○). Data represent the means \pm S.E.M. (n = 9-10/group).

Table 1. Effect of Rg₃ on wild-type and various mutant Na⁺ channels expressed in *Xenopus* oocytes

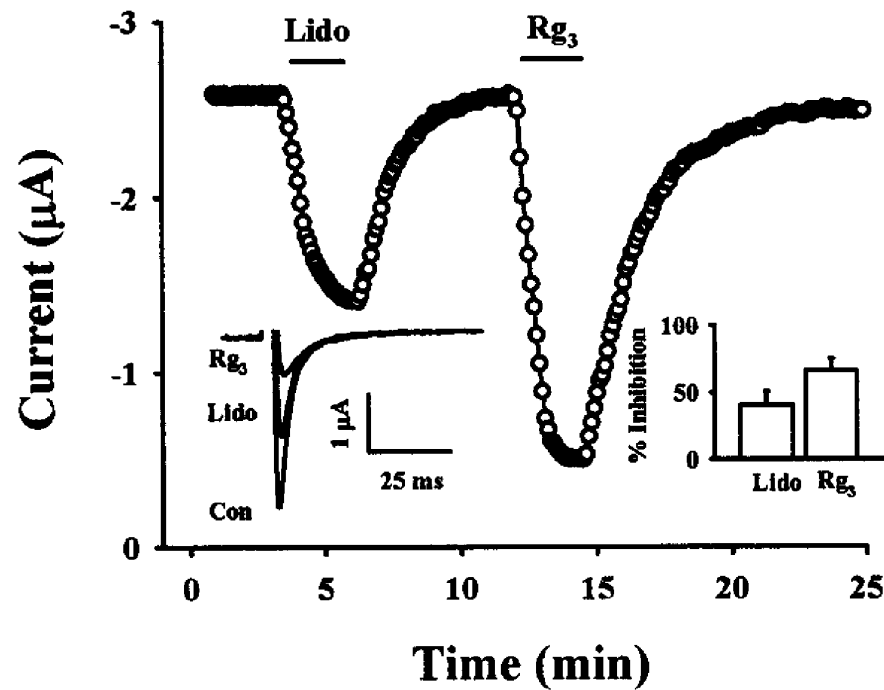
Type		IC ₅₀	n H	V _{max}
Wild		32 ± 6	1.1 ± 0.4	75 ± 6
Pore entrance				
	Y401C	43 ± 2*	1.5 ± 0.5	72 ± 2
	Y401T	22 ± 5	1.3 ± 0.3	61 ± 5
Channel pore				
	D927N	33 ± 4	1.1 ± 0.1	74 ± 3
	E942Q	40 ± 9	1.3 ± 0.3	58 ± 6
	E945Q	35 ± 5	1.2 ± 0.1	72 ± 4
Lidocaine binding site				
	F1764A	23 ± 4	1.3 ± 0.4	71 ± 3
	Y1771A	36 ± 6	1.1 ± 0.5	67 ± 5
	F1764A-Y1771A	33 ± 5	1.2 ± 0.1	70 ± 3
TTX binding site				
	F385C	26 ± 6	1.4 ± 0.4	52 ± 5
	F385S	27 ± 3	1.4 ± 0.2	73 ± 3
	F385Y	29 ± 9	1.2 ± 0.5	60 ± 9
	F385T	26 ± 8	1.0 ± 0.5	67 ± 9
	F385M	60 ± 6*	0.9 ± 0.4	84 ± 3
	E387G	36 ± 4	1.2 ± 0.1	85 ± 3
	E387T	29 ± 2	1.3 ± 0.4	60 ± 2
	E387Q	44 ± 9*	1.1 ± 0.2	75 ± 6
Voltage-Sensor				
Domain I	K226Q	30 ± 3	1.4 ± 0.2	65 ± 3
Domain II	K859Q	47 ± 9*	1.1 ± 0.1	88 ± 7
Domain III	R1312Q	30 ± 2	1.2 ± 0.7	73 ± 2
Domain IV	R1638Q	33 ± 6	1.0 ± 0.7	62 ± 3
Inactivation site				
IFMQ3	Peak	38 ± 3	1.1 ± 0.1	70 ± 5
	Plateau	14 ± 4	1.3 ± 0.4	98 ± 1
IFMQ3-K859Q	Peak	56 ± 6**	1.1 ± 0.3	76 ± 6
	Plateau	20 ± 1	1.4 ± 0.3	97 ± 2

Data represent mean ± S.E.M.(n=10-11/group). Currents were elicited by single-step voltage pulses from -100 mV to -10 mV at 0.2 Hz. *P<0.01, compared to wild-type Na⁺ channel. **P<0.01, compared to IFMQ3 mutant. The IC₅₀, Hill coefficient, and V_{max} values were determined as described in experimental procedures.

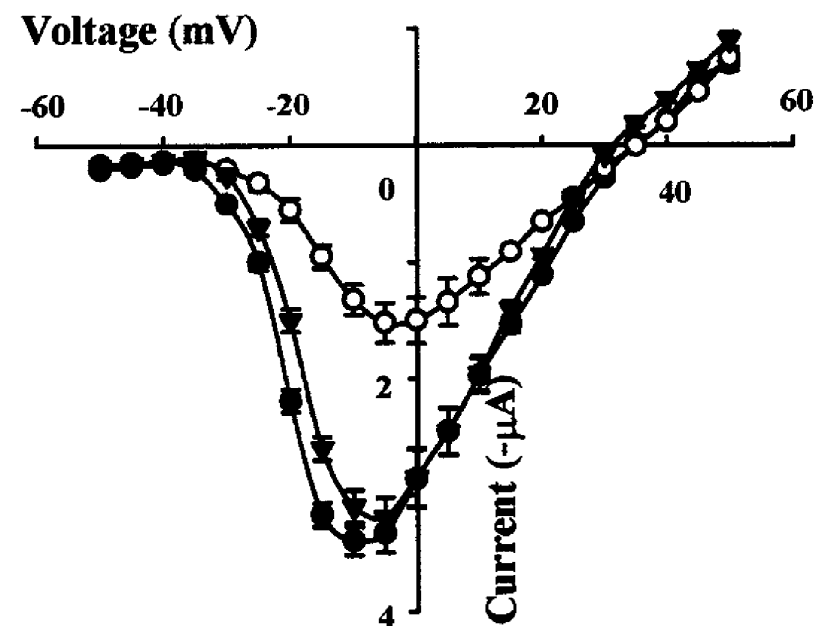


20(*S*)-Ginsenoside Rg₃

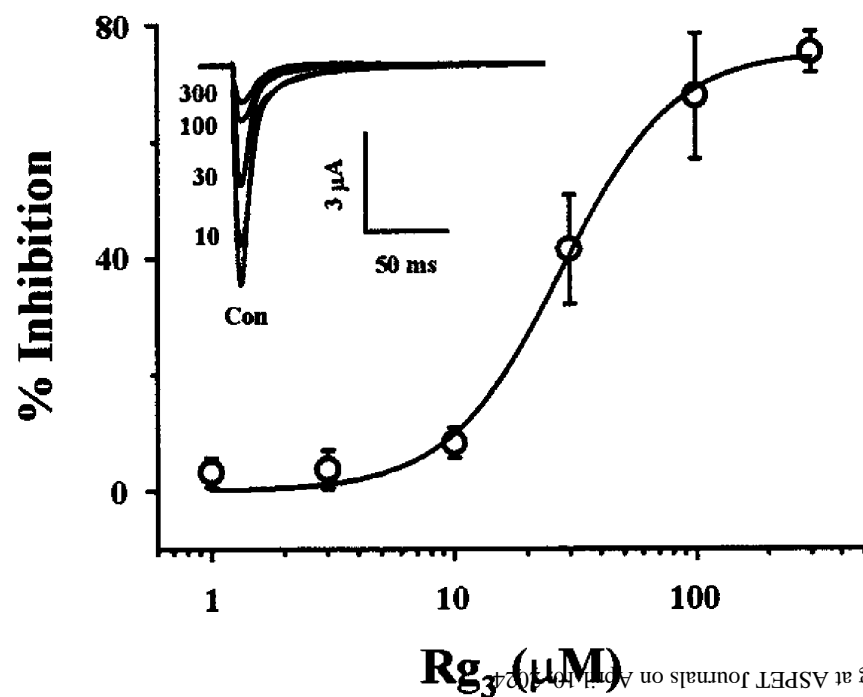
A



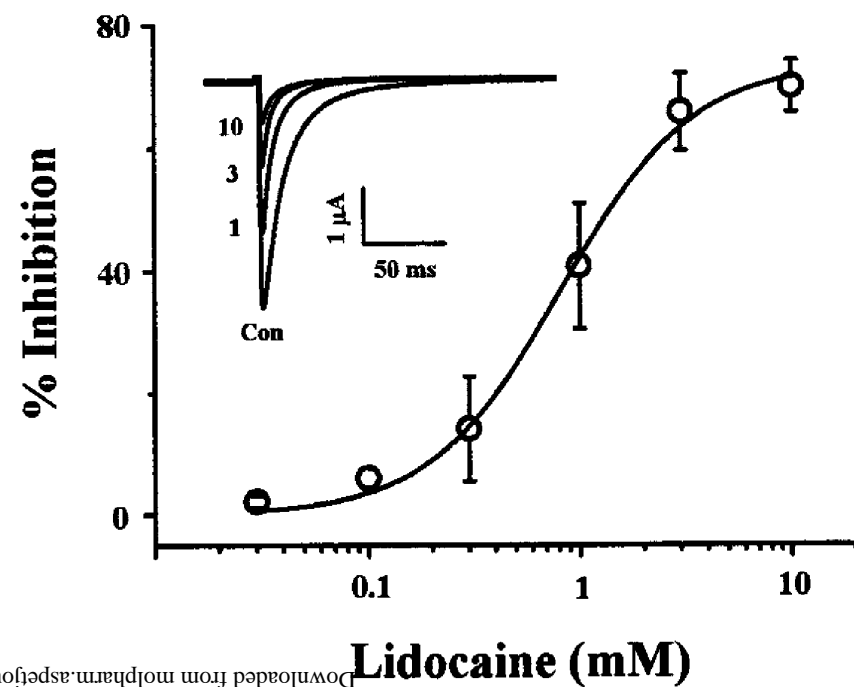
B



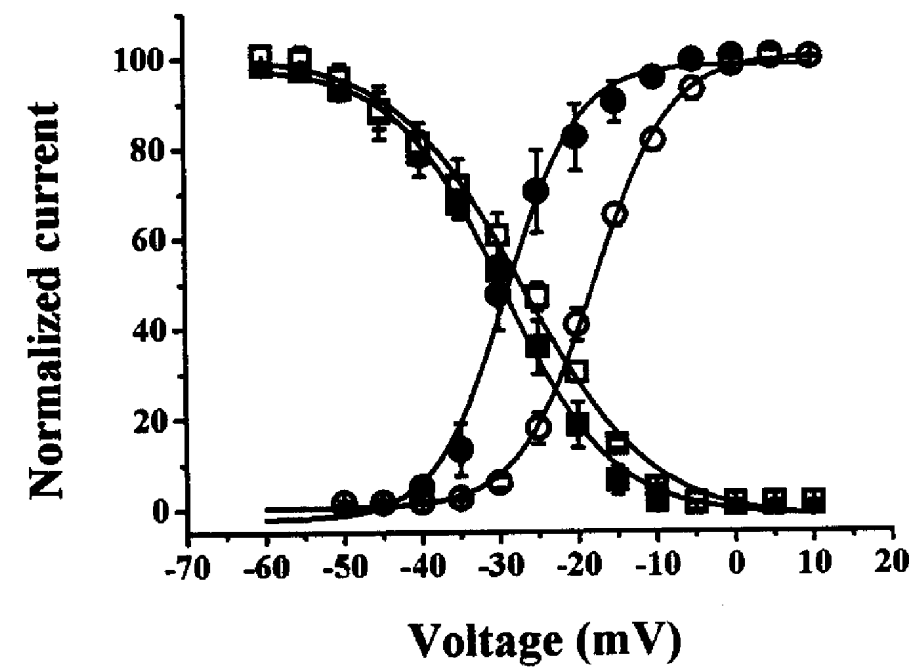
C



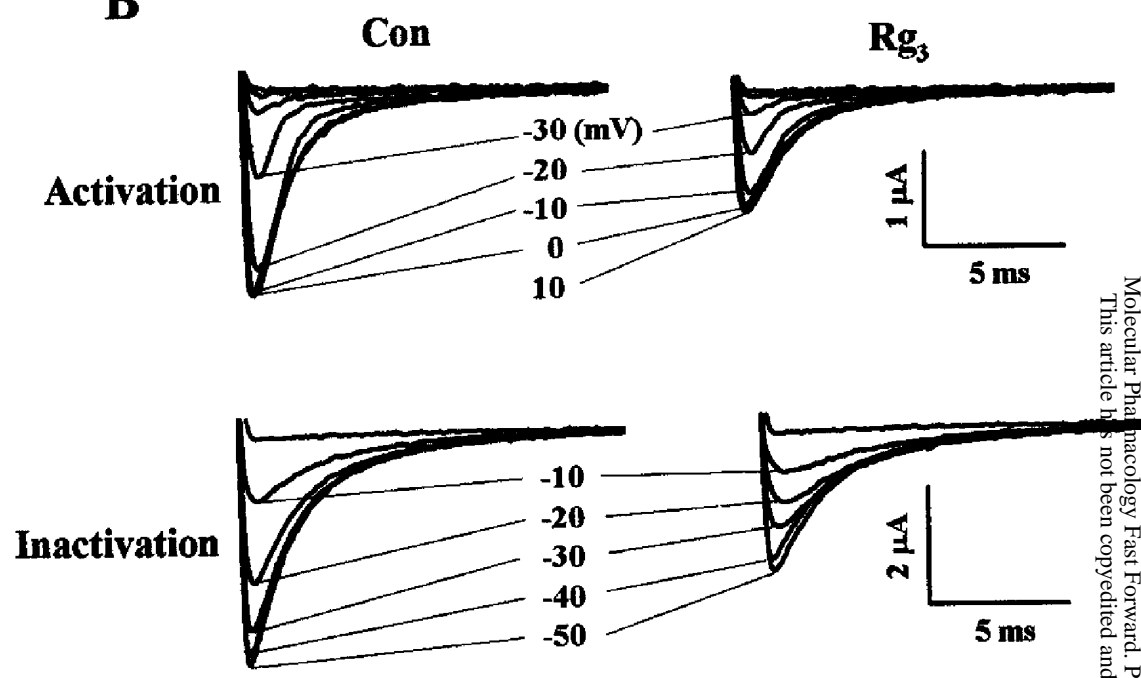
D



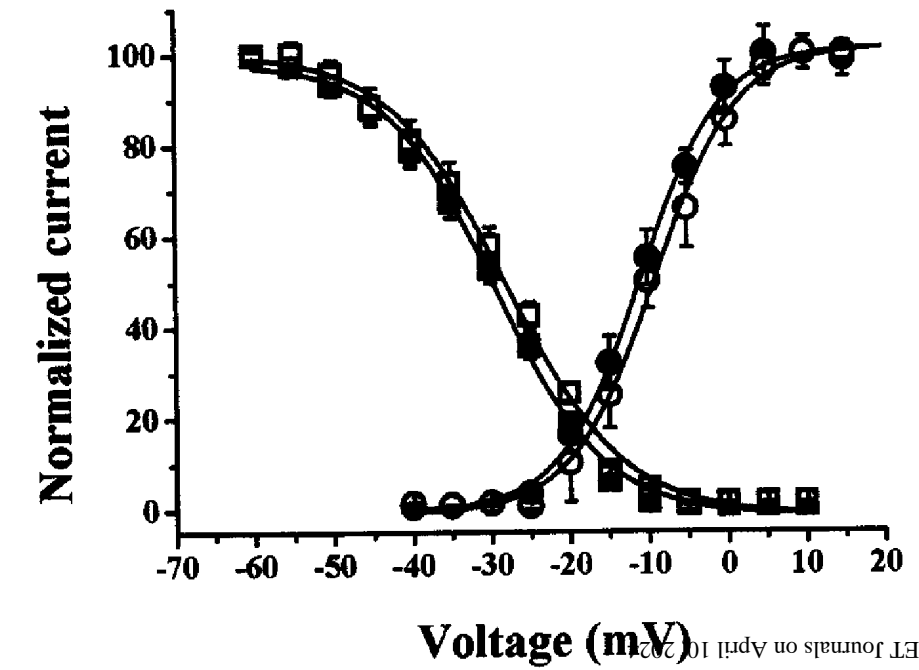
A. Wild-type



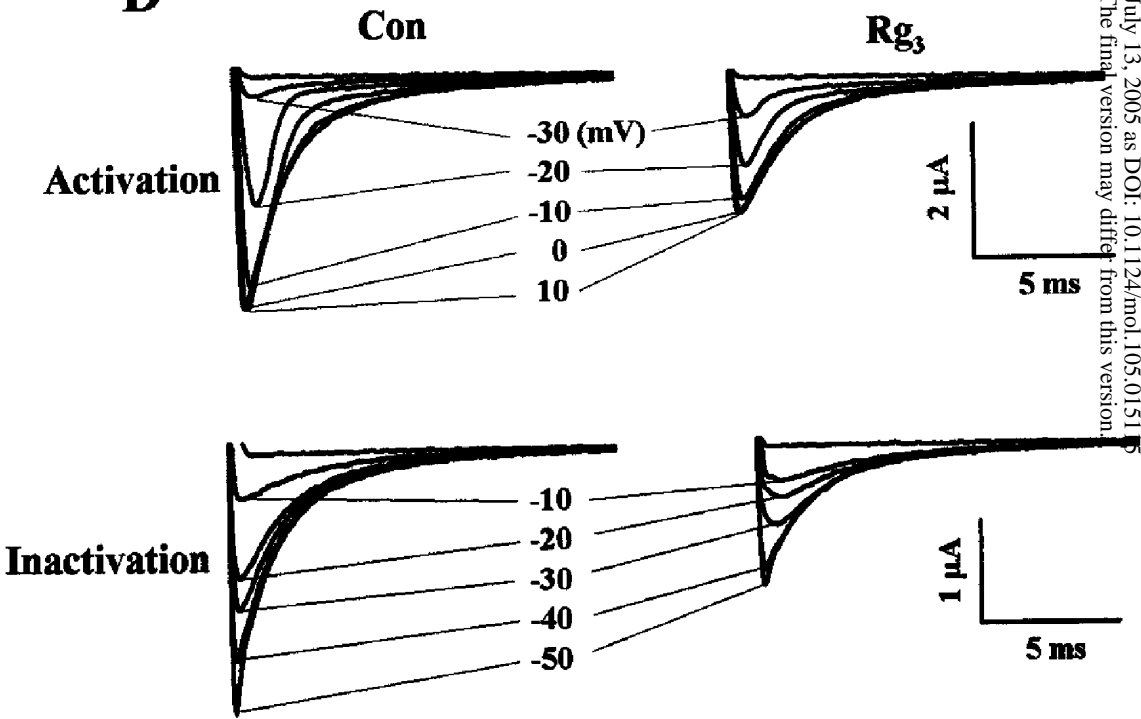
B



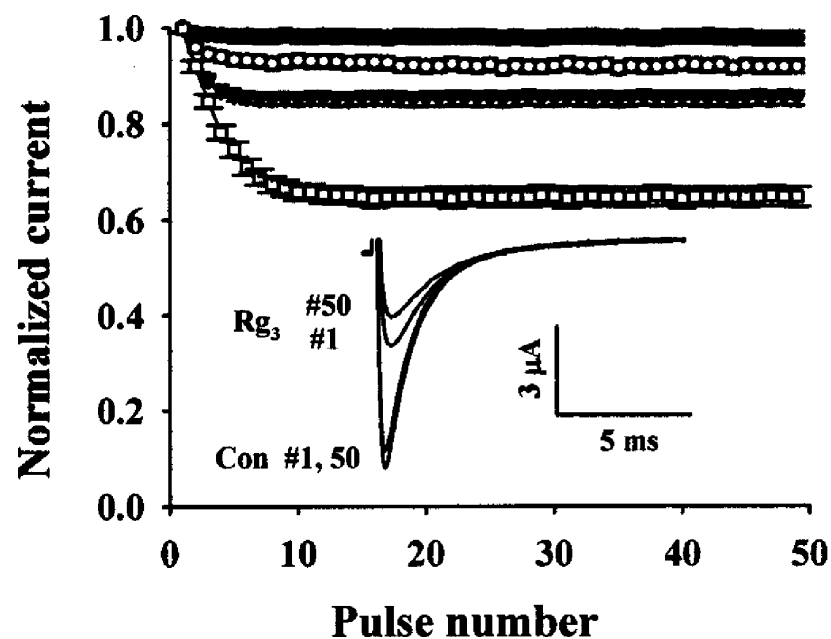
C. K859Q



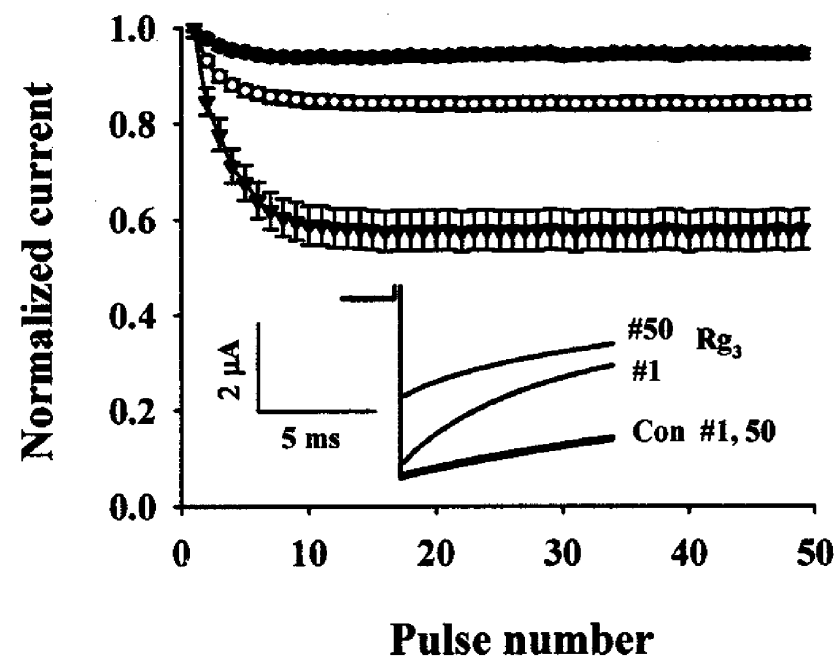
D



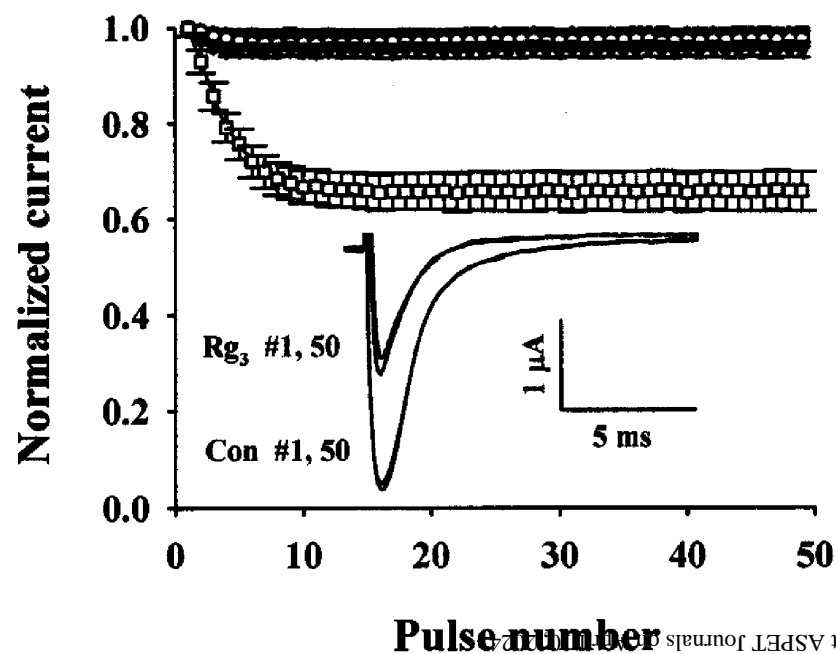
A. Wild-type



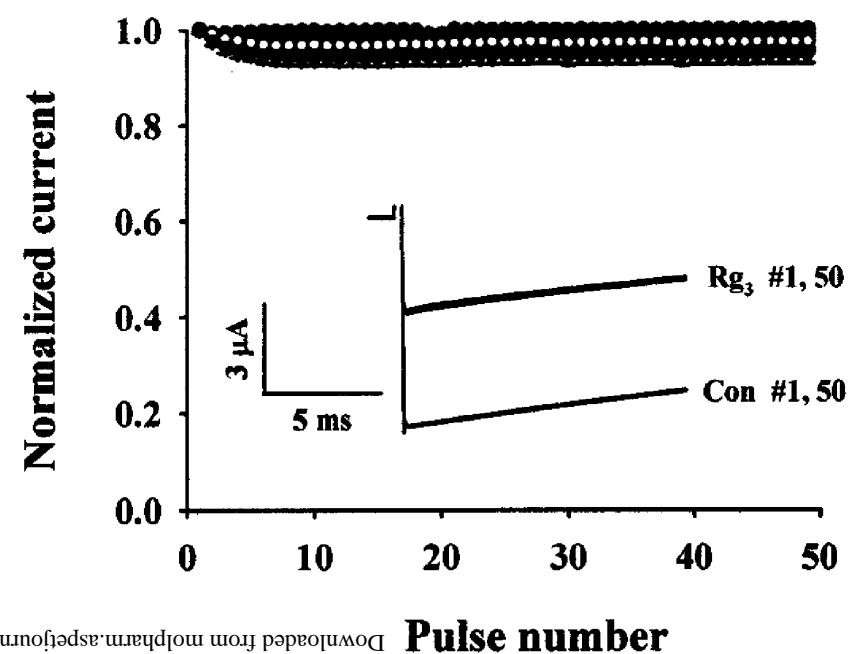
B. IFMQ3

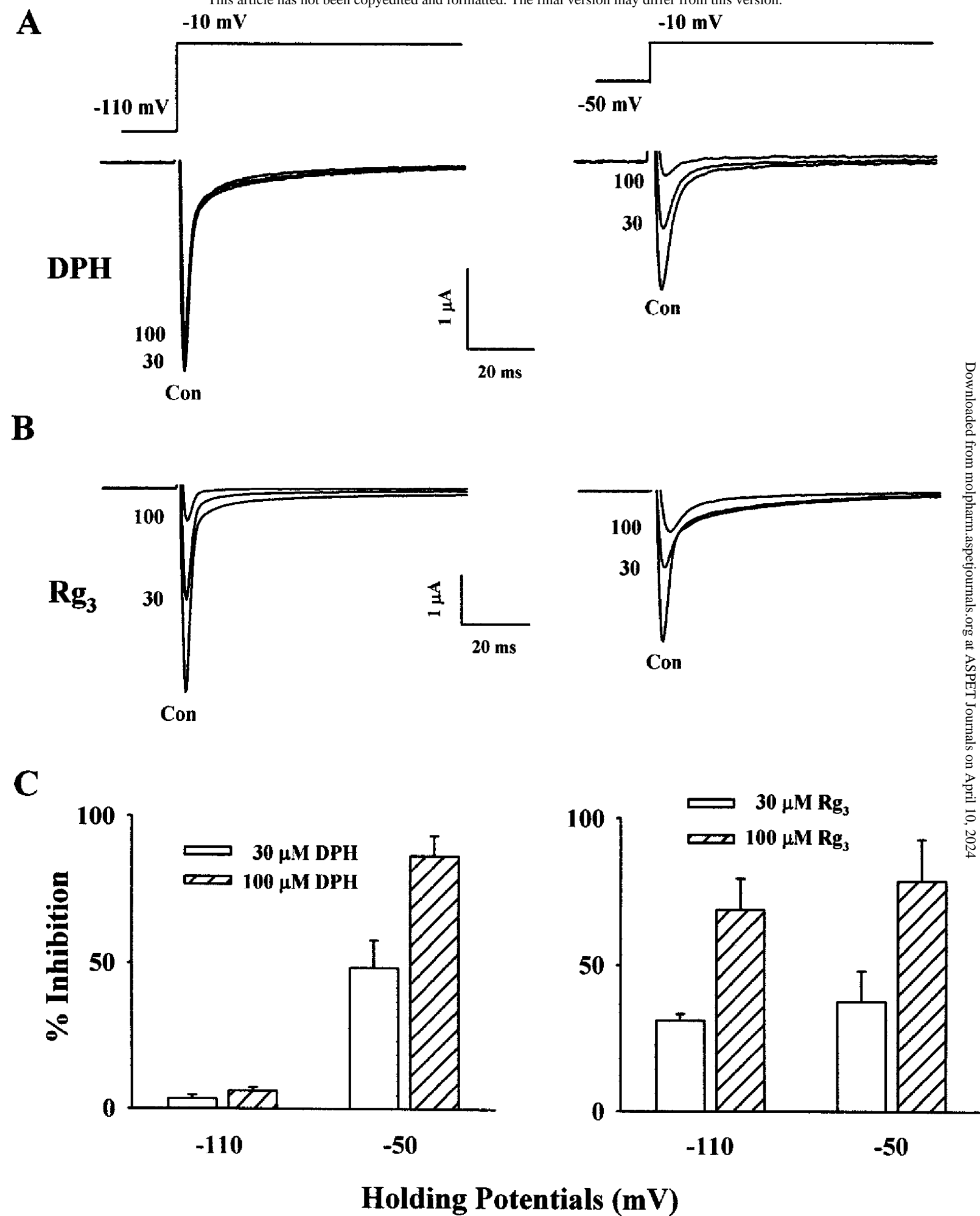


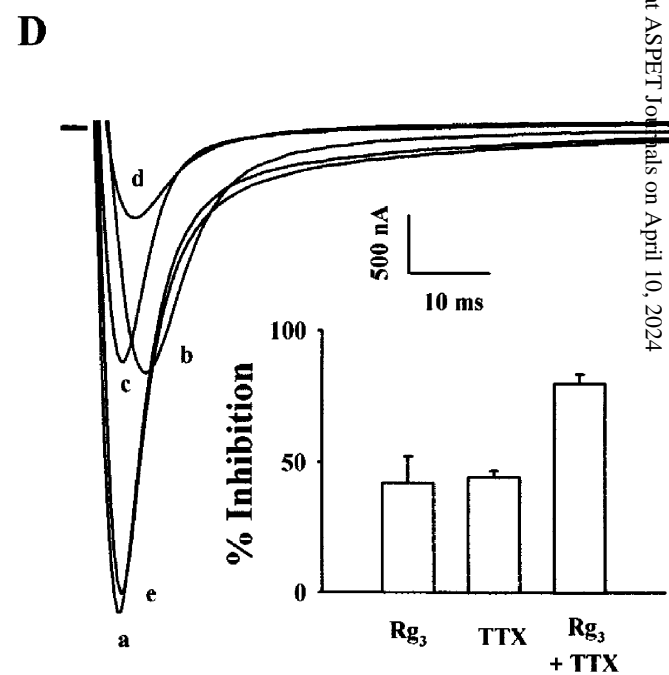
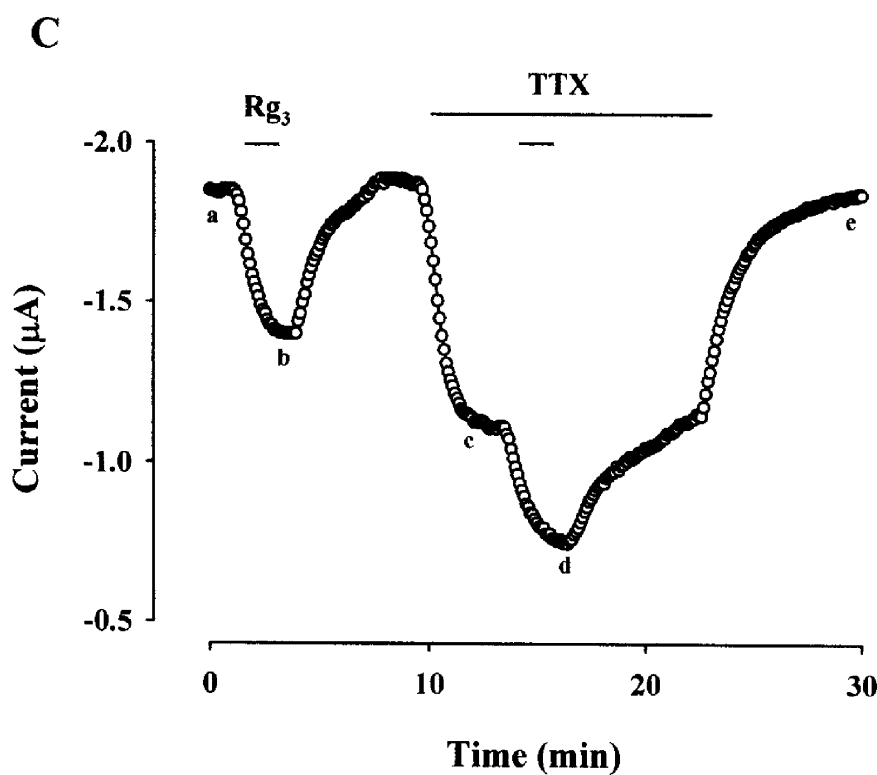
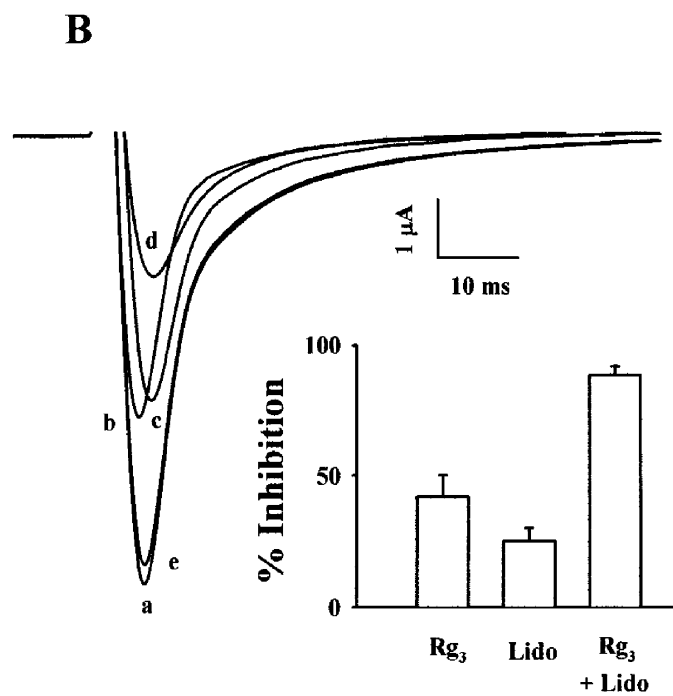
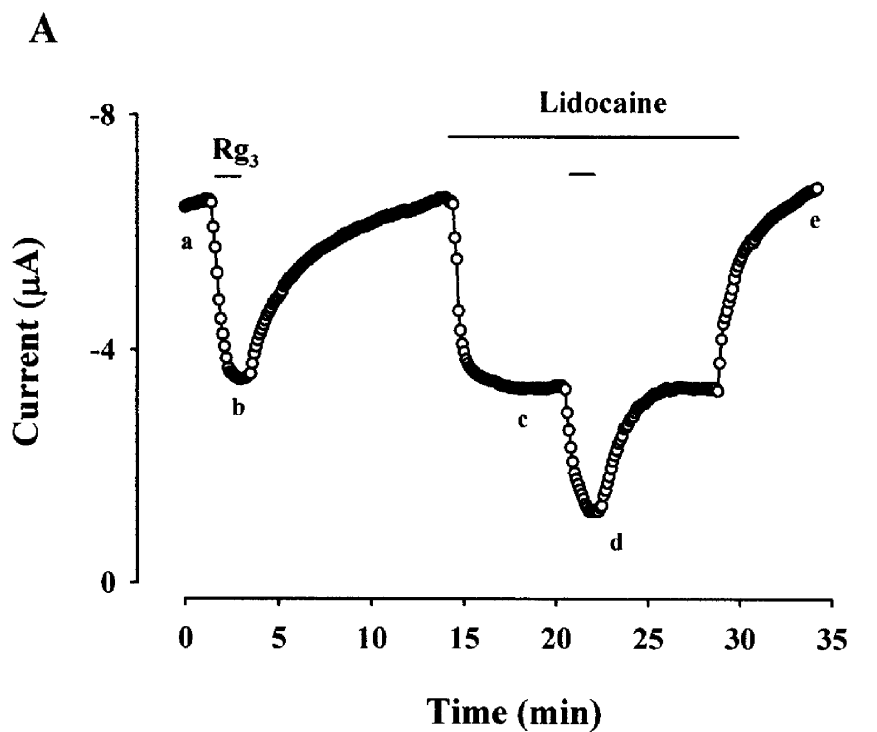
C. K859Q

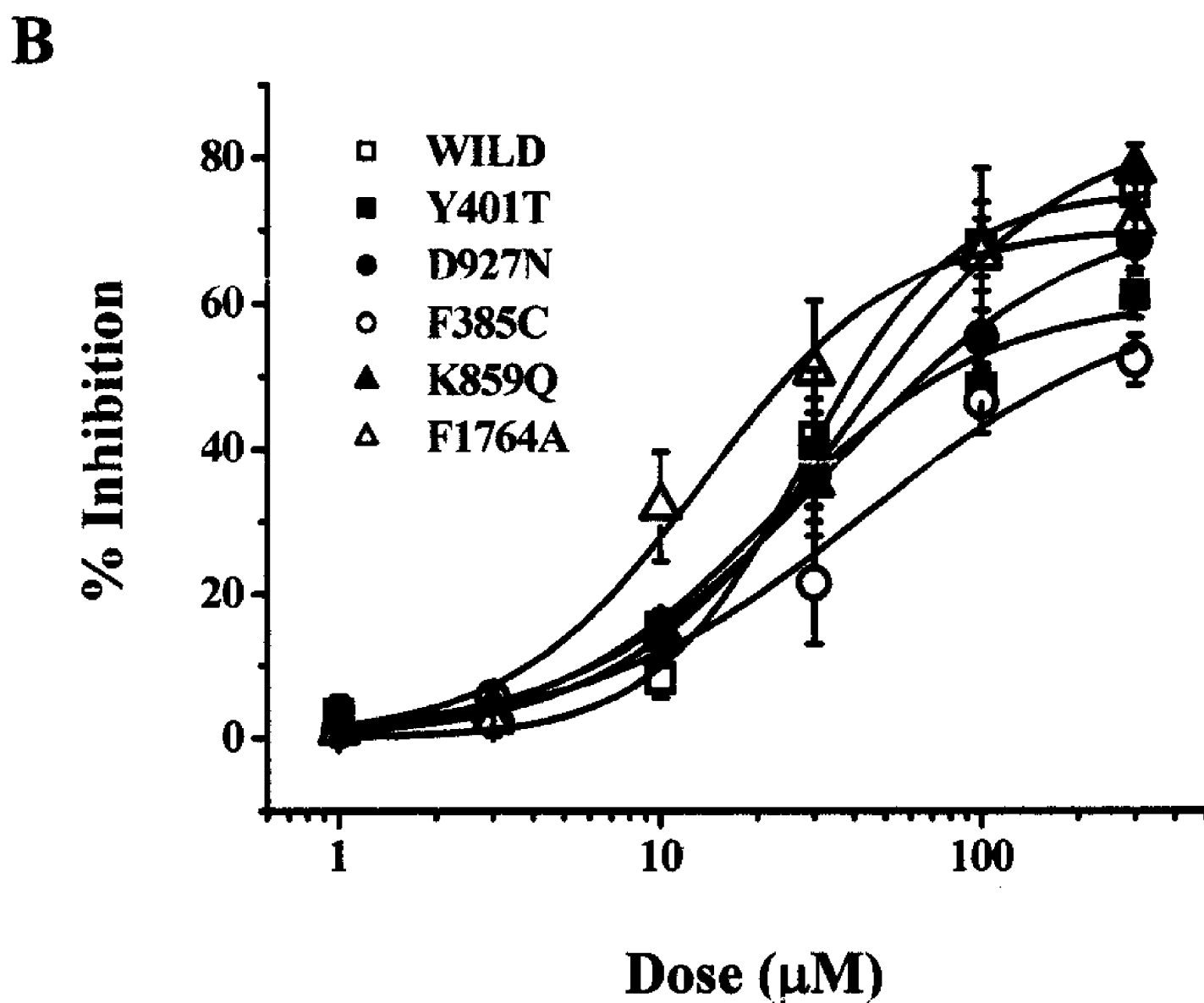
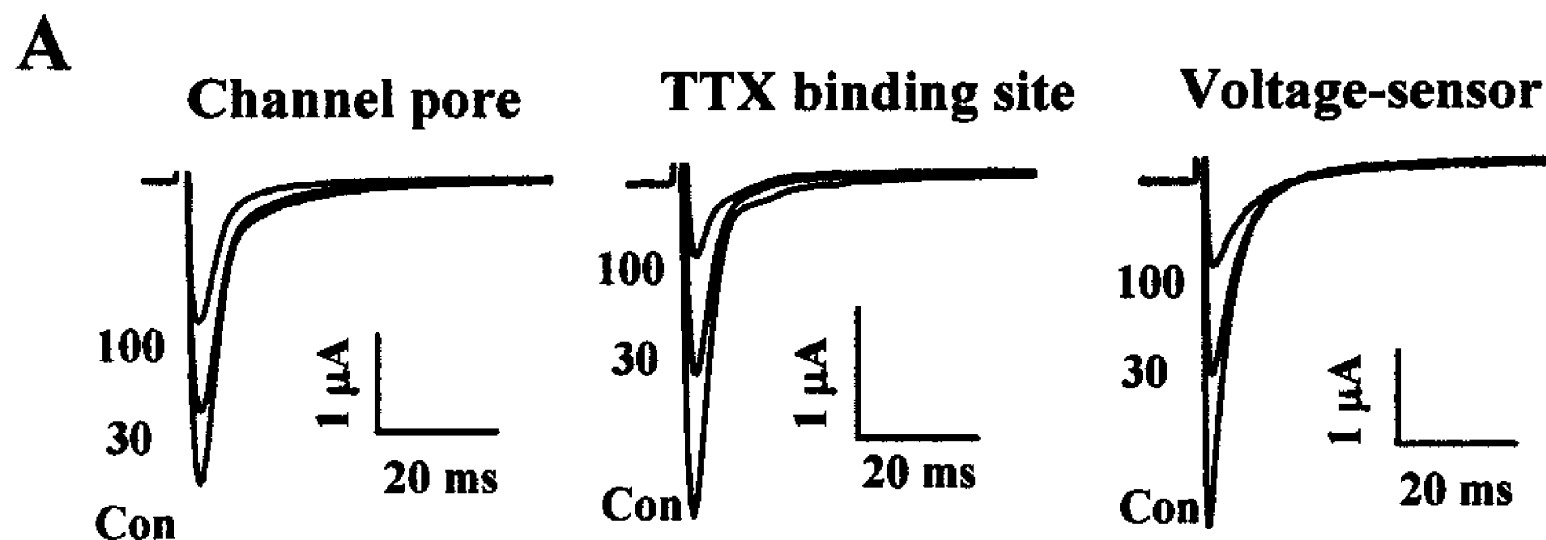


D. IFMQ3-K859Q



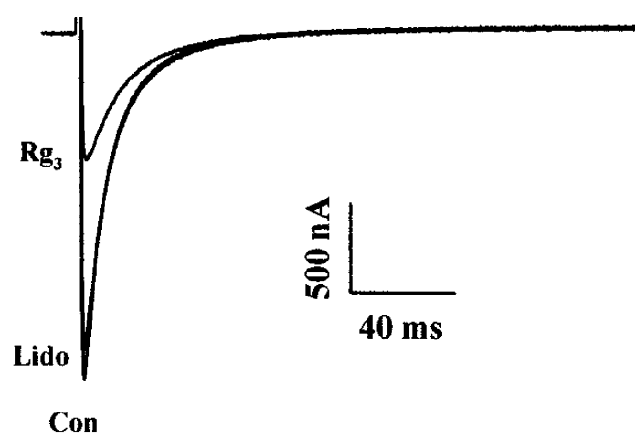




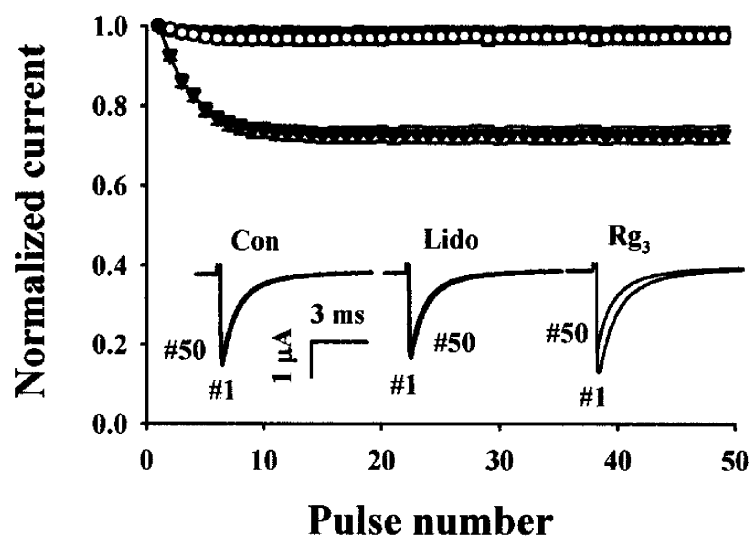


A. F1764A

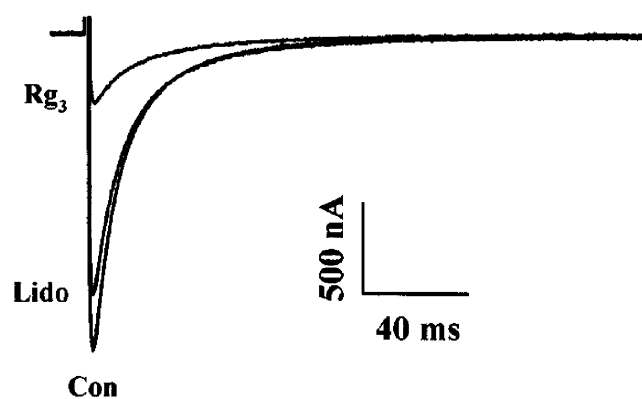
Molecular Pharmacology Fast Forward. Published on July 10, 2024 as DOI: 10.1124/mol.105.015115
This article has not been copyedited and formatted. The final version may differ from this version.



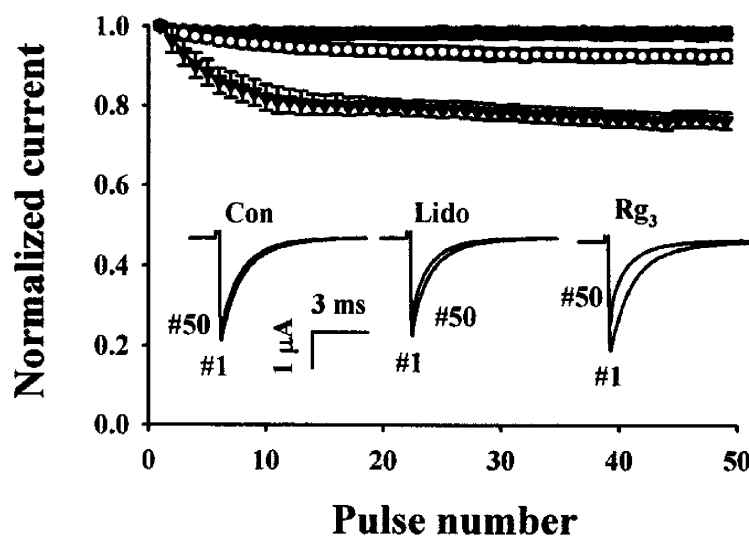
B. F1764A



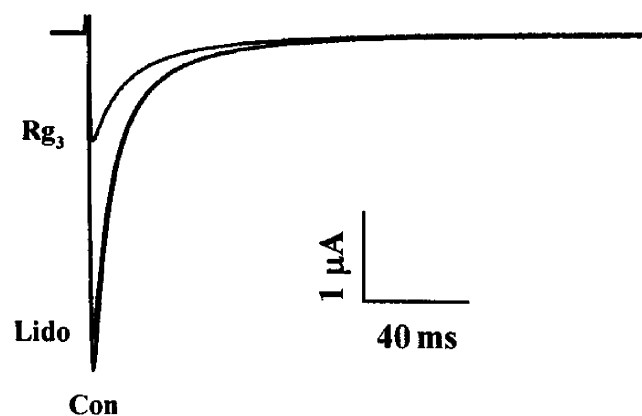
C. Y1771A



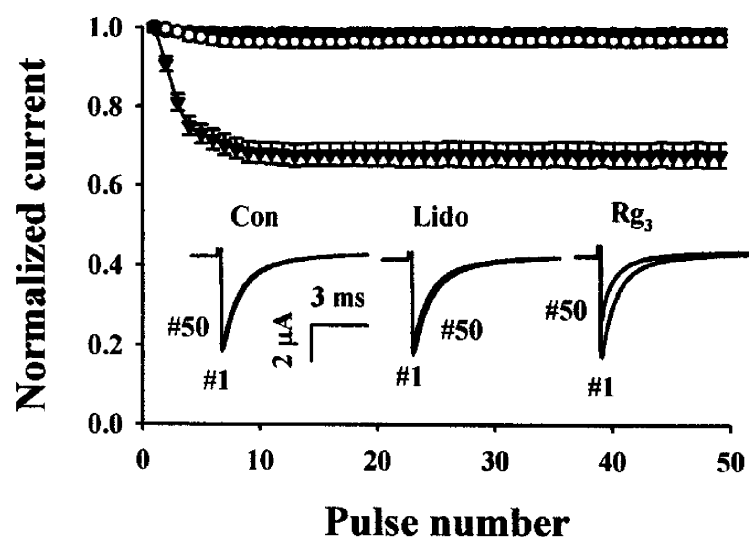
D. Y1771A



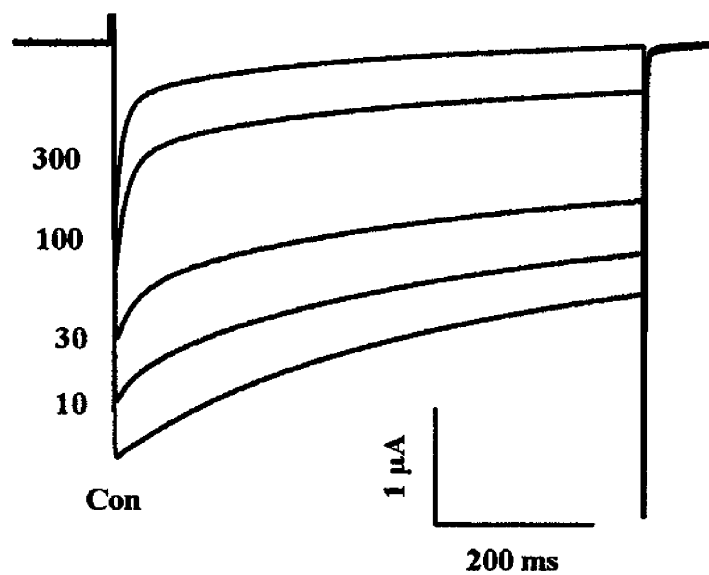
E. F1764A-Y1771A



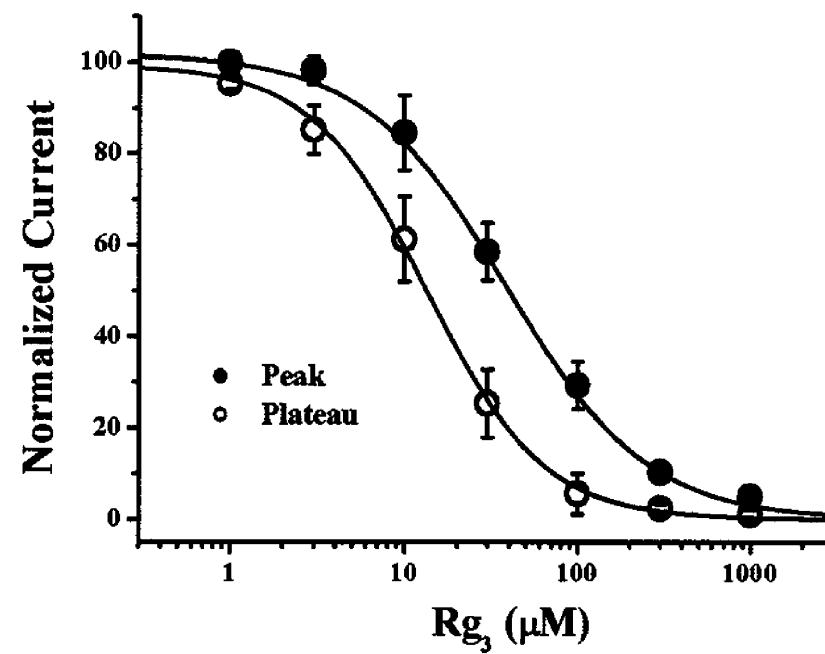
F. F1764A-Y1771A



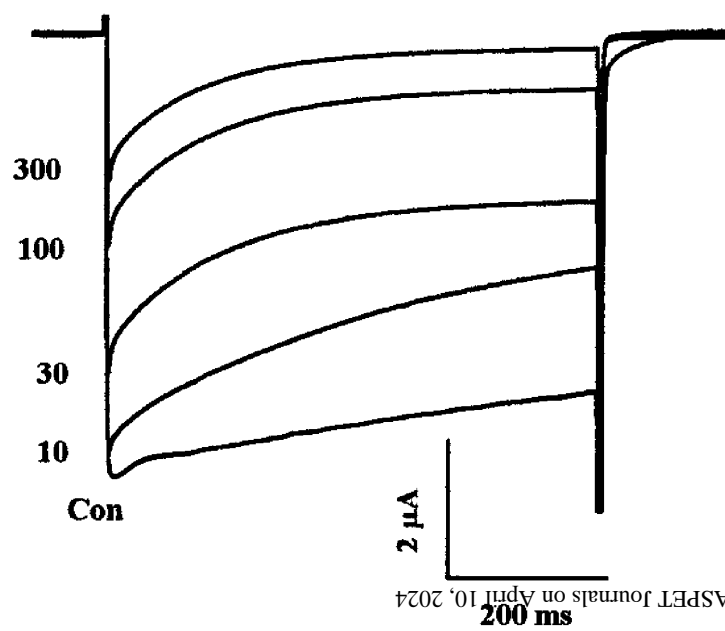
A



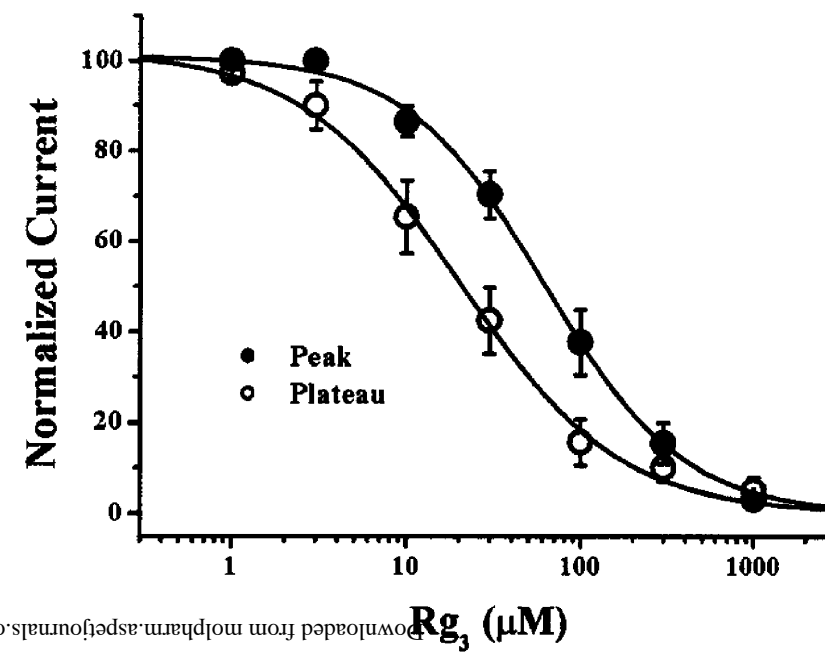
B



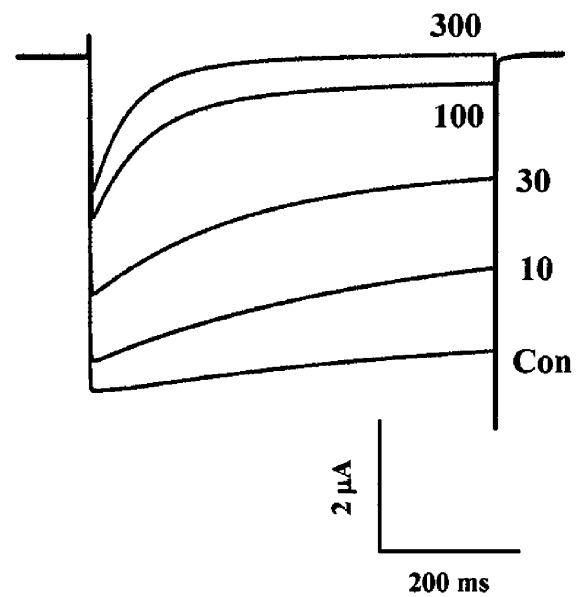
C



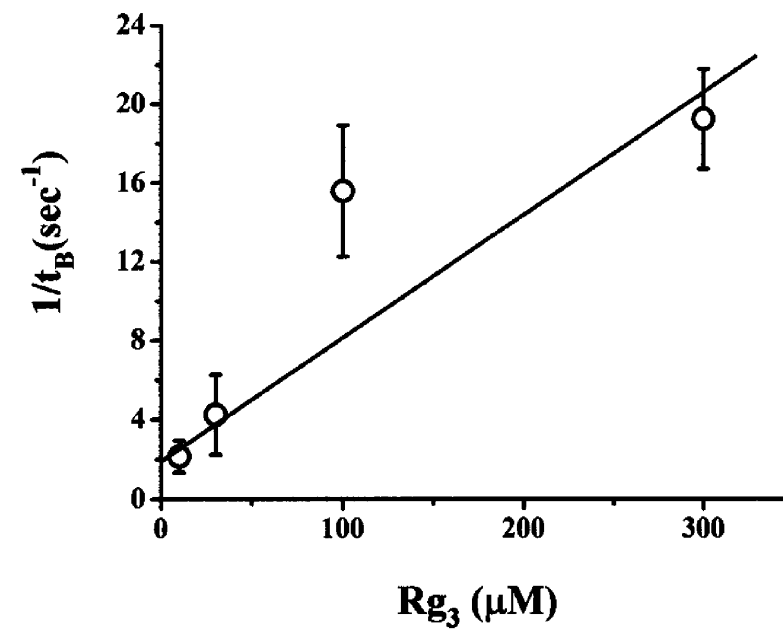
D



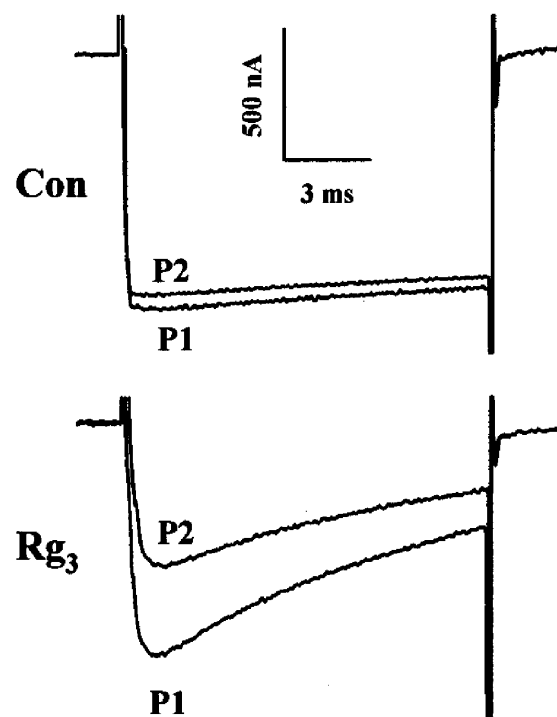
A



B



C



D

